Berry Phase in Atom Optics

Dissertation
zur Erlangung des akademischen Grades
Dr. rer. nat.
der Fakultät für Naturwissenschaften
der Universität Ulm

vorgelegt von
Polina V. Mironova
aus Woronesch

Institut für Quantenphysik
Direktor: Professor Dr. Wolfgang P. Schleich

Ulm, Dezember 2010

Amtierender Dekan: Prof. Dr. Axel Groß

Erstgutachter: Prof. Dr. Wolfgang P. Schleich
Zweitgutachter: Prof. Dr. Susana F. Huelga

Tag der Promotion: 23. Februar 2011

Contents

Introduction **5**

1 Berry Phase: a short review **9**
1.1 Adiabaticity in quantum mechanics 9
1.2 Berry phase: cyclic adiabatic geometric phase 12

2 Atom-field interaction: a brief summary **17**
2.1 The Hamiltonian of the atom-field interaction 17
2.2 Inverse cosh-envelope: exact solution 19

3 Atom optics and Berry phase **23**
3.1 Atomic scattering: standing wave 23
3.1.1 Set-up 23
3.1.2 Explicit expression for interaction matrix element 26
3.2 Dynamical and geometric phases 28
3.2.1 Connection to Berry's formulation 28
3.2.2 Connection between dressed states and atomic states 29
3.3 Circuit in parameter space 31
3.4 Explicit expressions for phases 33
3.4.1 Geometric phase 33
3.4.2 Dynamical phase 38
3.4.3 Ratio γ/β in possible experiment 40
3.5 Cancellation of the dynamical phase 41
3.6 Atomic lens based on the Berry phase 42

4 Alternative approaches **47**
4.1 WKB approach in the adiabatic case 47
4.2 Berry's approach and atomic state method: A comparison 51

5 Scattering from a traveling wave **55**
5.1 Schrödinger equation 55

5.2 Transition to Berry's formalism 57
5.2.1 Geometric and dynamical phases 58
5.2.2 Ratio $\gamma^{(r)}/\beta^{(r)}$ in possible experiment 60
5.2.3 Cancellation of the dynamical phase 60
5.3 Exact solution: $1/\cosh$ envelope 61
5.4 Comparison 63

Conclusion **65**

A Flux through infinitely many windings **69**

Bibliography **72**

Zusammenfassung **79**

Publications **81**

Posters and Talks **83**

Danksagung **85**

Introduction

The geometric phase [1–13] manifests itself in many different phenomena of physics ranging from the polarization change in the propagation of light in fibers [14, 15] via the precession of a neutron in a magnetic field [16–24], to the quantum dynamics of dark states in an atom [25]. Most recently, the geometric phase has also been used in topological quantum computing [26] as realized with trapped ions [27]. In the present thesis we propose a scheme to observe the geometric phase in the context of atom optics.

Brief review of geometric phase

The concept of the geometric phase arises in the context of a Hamiltonian dependent on the parameters which are slowly varying in time. When these variations are cyclic, that is the Hamiltonian returns to its initial form the instantaneous eigenstate will not necessarily regain its original value, but will pick up a phase. This phenomenon has been observed in experiments with polarized light, radio waves, molecules, etc. The most prominent example is the well-known Aharonov-Bohm effect, which was observed in 1959 [28] and explained in terms of the geometric phase 25 years later in the original paper by Berry [1]. Moreover, many familiar problems, such as the Foucault pendulum or the motion of a charged particle in a strong magnetic field, usually not associated with the Berry phase, might be explained elegantly in terms of it [3, 29–33].

Since the landmark paper on the geometric phase [1], extensive research, both theoretical and experimental , has been pursued on quantum holonomy [2, 3], adiabatic [14, 16, 34–39] and non-adiabatic [40, 41], cyclic [42] and non-cyclic [18, 43], Abelian [44] and non-Abelian [45, 46], as well as off-diagonal [17, 47] geometric phases. Moreover, geometric phase effects in the coherent excitation of a two-level atom have been identified [48–52]. Furthermore, geometric phases are rather insensitive to a particular kind of noise [19, 53] and therefore useful in the construction of robust quantum gates [26, 54–56]. Several proposals were given for the observation of the geometric phase in atom interferometry [25, 57, 58]. However, so far only the dependence on the atomic internal degrees of freedom was investigated. In the present thesis we extend this approach by taking into account atomic external degrees of freedom, that is the

center-of-mass-motion of the atom.

Our approach

We consider the scattering of a two-level atom from a near-resonant standing light wave. Within the Raman-Nath approximation [59] on the atomic center-of-mass motion, adiabatic turn-on and -off of the interaction together with the rotating wave approximation we obtain a condition for the cancellation of the dynamical phase and show that the scattering picture is determined only by the Berry phase dependent on the internal and external atomic degrees of freedom. Moreover, we propose a novel possibility to observe the Berry phase based on the atomic lens construction. This application of the Berry phase might even be useful in the realm of lithography with cold atoms.

The setup of our approach is the following. A two-level atom traverses a standing wave formed by two running waves with identical electric field amplitudes and frequencies. The propagation direction of the two waves is slightly different and the electromagnetic field is detuned with respect to the resonance frequency of the atom.

The key observation is that the dynamical phase is antisymmetric in the detuning, whereas the geometric phase is symmetric. As a result, a sequence of two such scattering arrangements which differ in the sign of their detunings must compensate the dynamical phase, but should double the geometric phase. In the present context we treat the center-of-mass motion parallel to the standing wave quantum mechanically. As a result the geometric phase imprinted on the internal state is position-dependent and can be observed by the intensity distribution of the atoms on a screen in the far field. This pattern corresponds to the momentum distributions of the atoms as they leave the second scattering zone.

Relation to earlier work

It is for three different reasons that our approach is different from earlier work on the Berry phase arising in the internal dynamics of the two-level atoms driven by laser fields: (i) in our scheme we compensate the dynamical phase; (ii) the geometric phase acquired by the internal states is imprinted on the center-of-mass motion of the atoms, and (iii) our setup does not require a traditional interference arrangement.

In a landmark experiment the dynamical phase of a neutron precessing in a magnetic field has been compensated [19] by an additional π-pulse. In our scheme this cancellation of the dynamical phase is achieved by changing the sign of the detuning as the atom moves from the first to the second scattering zone. The remarkable experiment [25] to observe the Berry phase in atomic system contained the geometric phase in the internal states only and was read out by an interferometry of these states. We

extend these ideas to atom optics where the center-of-mass motion is treated quantum mechanically. Here we take advantage of the entanglement between the internal atomic states and the external atomic center-of-mass motion, which allows us to read out the information about the geometric phase using the dynamics and the self-interference of the wave-packet.

Outline of the thesis

The thesis is organized as follows: After a brief review of the Berry phase in Ch. 1 and the basics of the atom-field interactions in Ch. 2, we formulate the problem addressed in the present thesis in Ch. 3.

In particular, we describe our setup and evaluate the Hamiltonian describing the interaction of the two-level atom with a standing wave in Sec. 3.1. We connect our model with the classic results of Berry and recall the expressions for the dynamical and geometric phases in Sec. 3.2. Here we emphasize the connection between the dressed and the atomic states. Since the geometric phase arises from the path in parameter space we construct in Sec. 3.3 for three different envelopes of the electric field the corresponding paths in the parameter space. Section 3.4 is devoted to the derivation of the explicit expressions for these phases. Here we concentrate on the weak field limit where the Rabi frequency is much smaller than the detuning. We find that the geometric phases in all three cases only differ by numerical factors. Sections 3.5 and 3.6 are dedicated to the discussion of the cancellation of the dynamical phase and the read out of the geometric phase with the help of the center-of-mass motion, respectively.

In Ch. 4 we introduce two alternative approaches of solving the problem addressed in the present thesis. We use the WKB method to rederive the dynamical and geometric phase for a two-level atom, as shown in Sec. 4.1. In Sec. 4.2 we make a comparison between the geometrical phase approach used in Ch. 3 and the atomic state approach.

We enlarge our analysis of the Berry phase in atom optics in Ch. 5 by considering the case of atomic scattering by the traveling wave, were we take the kinetic energy operator into account. Here we present the exact solution, easy to derive in the case of the inverse-cosh envelope of the electromagnetic field, and show that it is the same as the result derived within the Berry's approach, which, however, is easy to derive for any field envelope and therefore is much more generally applicable.

We summarize our main results in the Conclusion.

In order to keep the thesis self-contained we have included the calculations in the appendix. To evaluate the geometric phase for an electromagnetic beam which smoothly switches-on and switches-off the path in parameter space winds many times around the origin. In Appendix A we calculate the flux through these infinitely many windings.

Chapter 1

Berry Phase: a short review

Corresponding to the particular time dependence of the Hamiltonian, e.g. slowly varying, or rapidly varying, different methods for treating the system could be developed, that is adiabatic and sudden approximation, respectively.

For the slowly varying Hamiltonian, one can approximate the solutions of the Schrödinger equation by the stationary eigenfunctions of the instantaneous Hamiltonian, giving that a particular eigenfunction at one time goes over continuously into the corresponding eigenfunction at a later time.

1.1 Adiabaticity in quantum mechanics

In the following chapter we are going to recall the origin of the geometric phase, starting from the *Adiabatic Hypothesis* of Paul Ehrenfest [60] in old quantum mechanics, through the adiabatic theorem proved by Max Born and Vladimir Fock in 1928 [61] to the proposal of Sir Michael Berry in 1984 [1].

Adiabatic theorem: Ehrenfest's Hypothesis; Born and Fock

In 1913 Ehrenfest formulated his famous *Adiabatic Hypothesis* [60, 62, 63] and demonstrated the importance of adiabatic invariants [64]. "If a system be affected in a reversible adiabatic way, allowed motions are transformed into allowed motions" [62]. This heuristic principle together with Bohr's *Principle of Correspondence* have guided old quantum mechanics [62]. It was followed in the new quantum mechanics by the *Adiabatic theorem* [65].

In 1928 Born and Fock published a paper [61, 66] in which they proved the *Adiabatic theorem* as we know it today. If a system being initially in one of the eigenstates undergoes an adiabatic change then the probability of a transition into another eigenstate is infinitesimal.

Adiabatic approximation

Our review of the adiabatic theorem will follow the textbook [67] by Schiff.

Let us consider the time-dependent Schrödinger equation

$$i\hbar\frac{\partial\psi}{\partial t} = \hat{H}(t)\psi. \tag{1.1}$$

If we solve the corresponding eigenvalue equation

$$\hat{H}(t)u_n(t) = E_n(t)u_n(t) \tag{1.2}$$

at each instant of time, we expect that a system being in a discrete non degenerate state $u_m(0)$ with energy $E_m(0)$ at time $t = 0$ would be in the state $u_m(t)$ with energy $E_m(t)$ at time t in the case of Hamiltonian $\hat{H}(t)$, which is slowly changing with time. Now we are able to expand the function ψ in terms of the eigenfunctions u_n,

$$\psi = \sum_n a_n(t)u_n(t)\exp\left[-\frac{\mathrm{i}}{\hbar}\int_0^t \mathrm{d}t'\, E_n(t')\right], \tag{1.3}$$

assuming that the basis u_n is orthonormal, discrete and non degenerate, that is

$$\int \mathrm{d}^3r\, u_n^* u_m = \delta_{n,m}. \tag{1.4}$$

Substituting the expansion of the function ψ, Eq. (1.3), into the time-dependent Schrödinger equation (1.1) and taking into account the "instantaneous" stationary Schrödinger equation (1.2) we arrive at

$$\sum_n \left(\dot{a}_n u_n + a_n\dot{u}_n\right)\exp\left[-\frac{i}{\hbar}\int_0^t \mathrm{d}t'\, E_n(t')\right] = 0. \tag{1.5}$$

Multiplying Eq. (1.5) by u_k^* on the left and integrating over all space, we obtain

$$\dot{a}_k = -\sum_n a_n \exp\left\{-\frac{i}{\hbar}\int_0^t \mathrm{d}t'\ [E_n(t') - E_k(t')]\right\}\int \mathrm{d}^3r\, u_k^*\dot{u}_n. \tag{1.6}$$

In order to derive the matrix element $\int \mathrm{d}^3r\, u_k^*\dot{u}_n$, assuming $k \neq n$, we differentiate the stationary Schrödinger equation (1.2) over time t

$$\frac{\partial\hat{H}}{\partial t}u_n + \hat{H}\frac{\partial}{\partial t}u_n = \frac{\partial E_n}{\partial t}u_n + E_n\frac{\partial}{\partial t}u_n \tag{1.7}$$

then multiply the obtained equation by u_k^* on the left and integrate over all space, giving

$$\int \mathrm{d}^3r\, u_k^*\dot{u}_n = \frac{1}{E_n - E_k}\int \mathrm{d}^3r\, u_k^*\frac{\partial\hat{H}}{\partial t}u_n. \tag{1.8}$$

To obtain the expression for $\int \mathrm{d}^3r\, u_n^* \dot{u}_n$ we differentiate the orthonormality condition $\int \mathrm{d}^3r\, u_n^* u_n = 1$ with respect to time

$$\int \mathrm{d}^3r\, u_n^* \dot{u}_n + \int \mathrm{d}^3r\, \dot{u}_n^* u_n = 2\mathrm{Re} \int \mathrm{d}^3r\, u_n^* \dot{u}_n = 0, \tag{1.9}$$

which reflects the purely imaginary nature of $\int \mathrm{d}^3r\, u_n^* \dot{u}_n \equiv \mathrm{i}\alpha_n(t)$, where $\alpha_n(t)$ is some real-valued time-dependent function.

Using the fact, that the phases of the states u_n are not determined unambiguously, but might be chosen arbitrary, we consider a state $u'_n \equiv u_n \exp[\mathrm{i}\gamma_n(t)]$ and obtain

$$\int \mathrm{d}^3r\, {u'_n}^* \dot{u}'_n = \int \mathrm{d}^3r\, u_n^* \dot{u}_n + i\dot{\gamma}_n = i(\alpha_n + \dot{\gamma}_n). \tag{1.10}$$

Therefore, we can put all the expressions $\int \mathrm{d}^3r\, {u'_n}^* \dot{u}'_n = 0$ by the choice $\dot{\gamma}_n = -\alpha_n$, valid for all n. Let us assume that the choice of all the phases were made in the above-presented way and omit the primes.

Substituting the equation for the matrix element $\int \mathrm{d}^3r\, u_k^* \dot{u}_n$, Eq. (1.8), into the equation for the amplitude a_k, Eq. (1.6), we obtain

$$\dot{a}_k = -\sum_{n \neq k} \frac{a_n}{E_n - E_k} \exp\left\{ -\frac{i}{\hbar} \int_0^t \mathrm{d}t' \left[E_n(t') - E_k(t') \right] \right\} \int \mathrm{d}^3r\, u_k^* \frac{\partial \hat{H}}{\partial t} u_n, \tag{1.11}$$

In order to obtain a qualitative understanding of the behavior of the probability amplitudes a_k, we assume all quantities on the right-hand side of Eq. (1.11) so slowly varying with time that we consider them constant. Moreover, we assume the system was in a well-defined initial state u_m at the time $t = 0$, which allow us to put $a_n \equiv \delta_{nm}$. Hence, we derive

$$\dot{a}_k \approx -\frac{1}{E_m - E_k} \exp\left[-\frac{i}{\hbar} (E_m - E_k)\, t \right] \int \mathrm{d}^3r\, u_k^* \frac{\partial \hat{H}}{\partial t} u_m, \tag{1.12}$$

Therefore, after the integration of Eq. (1.12) we obtain

$$a_k \approx \frac{\hbar}{\mathrm{i}(E_m - E_k)^2} \left\{ \exp\left[-\frac{i}{\hbar} (E_m - E_k)\, t \right] - 1 \right\} \int \mathrm{d}^3r\, u_k^* \frac{\partial \hat{H}}{\partial t} u_m \tag{1.13}$$

Thus, we show that the probability amplitudes a_k oscillate in time and does not increase steadily even when the Hamiltonian changes. Hence, the hypothesis of Ehrenfest [60, 63, 64] was proved in the adiabatic theorem by Born and Fock [61, 67]. Indeed, if the rate of change of Hamiltonian, $\partial \hat{H}/\partial t$, is negligibly small, the system remains in the instantaneous eigenstate and no transition to any other state can occur, as expressed by Eqs. (1.11) and (1.13). That is, the relation

$$\frac{1}{(E_m - E_k)^2} \frac{\partial \hat{H}}{\partial t} \to 0 \tag{1.14}$$

determines the condition of the adiabaticity.

1.2 Berry phase: cyclic adiabatic geometric phase

A particular feature of the adiabatic theorem, overlooked for decades, was revealed by Berry in 1984, when he attracted attention to the uninvestigated non-dynamical phase factor, which he named *the geometric phase* in his pioneering work [1]. This geometric phase factor, acquired in the case of the adiabatic cyclic evolution of the system with non-degenerate Hamiltonian, is well known now as *the Berry phase*. The adjective "geometric" arose from the fact that this phase depends only on the geometry of the parameter space, by which we understand a multi-dimensional hyper-space, formed by the changing parameters of the system.

Berry proposed to consider a system, whose Hamiltonian depends on some real-valued parameters, forming the multi-dimensional vector $\boldsymbol{\mathcal{R}}$ [1, 59]. Here we have chosen the calligraphic letter rather than the normal one in order to bring out the fact that the vector $\boldsymbol{\mathcal{R}}$ does not lie in three-dimensional real space but in the parameter space. These parameters are assumed to change slowly with time. Therefore, if the system was initially in one of the eigenstates of the Hamiltonian,

$$\hat{H}[\boldsymbol{\mathcal{R}}(t)]|u_n[\boldsymbol{\mathcal{R}}(t)]\rangle = \varepsilon_n[\boldsymbol{\mathcal{R}}(t)]|u_n[\boldsymbol{\mathcal{R}}(t)]\rangle \tag{1.15}$$

then during the adiabatic evolution with time it will remain in this instantaneous eigenstate. A state of the system can be described through the superposition of the eigenstates

$$|\Psi[\boldsymbol{\mathcal{R}}(t)]\rangle = \sum_m K_m[\boldsymbol{\mathcal{R}}(t)]|u_m[\boldsymbol{\mathcal{R}}(t)]\rangle, \tag{1.16}$$

where the coefficients $K_m[\boldsymbol{\mathcal{R}}(t)]$ can be determined by the projection onto the left eigenstates $\langle u_n[\boldsymbol{\mathcal{R}}(t)]|$. Substituting the state of the system Eq. (1.16) into the Schrödinger equation

$$\mathrm{i}\hbar\frac{\mathrm{d}}{\mathrm{d}t}|\Psi[\boldsymbol{\mathcal{R}}(t)]\rangle = \hat{H}[\boldsymbol{\mathcal{R}}(t)]|\Psi[\boldsymbol{\mathcal{R}}(t)]\rangle. \tag{1.17}$$

we obtain

$$i\hbar\sum_m\left[K_m[\boldsymbol{\mathcal{R}}(t)]\frac{d}{dt}|u_m[\boldsymbol{\mathcal{R}}(t)]\rangle + \frac{dK_m[\boldsymbol{\mathcal{R}}(t)]}{dt}|u_m[\boldsymbol{\mathcal{R}}(t)]\rangle\right] = \sum_m K_m[\boldsymbol{\mathcal{R}}(t)]\varepsilon_m|u_m[\boldsymbol{\mathcal{R}}(t)]\rangle. \tag{1.18}$$

Projecting Eq. (1.18) onto the left eigenstates $\langle u_n[\boldsymbol{\mathcal{R}}(t)]|$

$$\begin{aligned} &i\hbar\sum_m\left\{K_m[\boldsymbol{\mathcal{R}}(t)]\langle u_n[\boldsymbol{\mathcal{R}}(t)]|\frac{d}{dt}|u_m\rangle + \frac{dK_m[\boldsymbol{\mathcal{R}}(t)]}{dt}\langle u_n[\boldsymbol{\mathcal{R}}(t)]|u_m[\boldsymbol{\mathcal{R}}(t)]\rangle\right\} \\ &= \sum_m K_m[\boldsymbol{\mathcal{R}}(t)]\varepsilon_m\langle u_n[\boldsymbol{\mathcal{R}}(t)]|u_m[\boldsymbol{\mathcal{R}}(t)]\rangle \end{aligned} \tag{1.19}$$

and using the normalization condition

$$\langle u_m[\boldsymbol{\mathcal{R}}(t)]|u_n[\boldsymbol{\mathcal{R}}(t)]\rangle = \delta_{mn} \tag{1.20}$$

we obtain

$$\begin{aligned} i\hbar\dot{K}_n[\boldsymbol{\mathcal{R}}(t)] &= K_n[\boldsymbol{\mathcal{R}}(t)]\varepsilon_n - i\hbar K_n[\boldsymbol{\mathcal{R}}(t)]\langle u_n[\boldsymbol{\mathcal{R}}(t)]|\frac{d}{dt}|u_n[\boldsymbol{\mathcal{R}}(t)]\rangle \\ &\quad -i\hbar\sum_{m\neq n} K_m[\boldsymbol{\mathcal{R}}(t)]\langle u_n[\boldsymbol{\mathcal{R}}(t)]|\frac{d}{dt}|u_m[\boldsymbol{\mathcal{R}}(t)]\rangle. \end{aligned} \tag{1.21}$$

The last term of Eq. (1.21) can be neglected within the adiabatic approximation Eq. (1.14).

Now we change from the differentiation over time t to the differentiation over the parameters $\boldsymbol{\mathcal{R}}$

$$\frac{d}{dt}|u_n[\boldsymbol{\mathcal{R}}(t)]\rangle = \frac{\partial|u_n[\boldsymbol{\mathcal{R}}(t)]\rangle}{\partial\boldsymbol{\mathcal{R}}}\cdot\frac{d\boldsymbol{\mathcal{R}}}{dt} = \{\nabla_{\boldsymbol{\mathcal{R}}}|u_n[\boldsymbol{\mathcal{R}}(t)]\rangle\}\,\dot{\boldsymbol{\mathcal{R}}} \tag{1.22}$$

resulting in the equation

$$\dot{K}_n[\boldsymbol{\mathcal{R}}(t)] = -\frac{i}{\hbar}K_n[\boldsymbol{\mathcal{R}}(t)]\varepsilon_n - K_n[\boldsymbol{\mathcal{R}}(t)]\langle u_n[\boldsymbol{\mathcal{R}}(t)]|\nabla_{\boldsymbol{\mathcal{R}}}|u_n[\boldsymbol{\mathcal{R}}(t)]\rangle\dot{\boldsymbol{\mathcal{R}}}. \tag{1.23}$$

This equation has the solution

$$K_n[\boldsymbol{\mathcal{R}}(t)] = \exp\left\{-\frac{i}{\hbar}\int_0^t \varepsilon_n(t')dt' - \int_0^t \langle u_n(\boldsymbol{\mathcal{R}})|\nabla_{\boldsymbol{\mathcal{R}}}|u_n(\boldsymbol{\mathcal{R}})\rangle\dot{\boldsymbol{\mathcal{R}}}dt'\right\}K_n[\boldsymbol{\mathcal{R}}(0)] \tag{1.24}$$

or, applying the relation $\dot{\boldsymbol{\mathcal{R}}}dt \equiv d\boldsymbol{\mathcal{R}}$,

$$K_n[\boldsymbol{\mathcal{R}}(t)] = \exp\left\{-\frac{i}{\hbar}\int_0^t \varepsilon_n(t')dt' - \int_{\mathcal{L}(t)} \langle u_n(\boldsymbol{\mathcal{R}})|\nabla_{\boldsymbol{\mathcal{R}}}|u_n(\boldsymbol{\mathcal{R}})\rangle d\boldsymbol{\mathcal{R}}\right\}K_n[\boldsymbol{\mathcal{R}}(0)], \tag{1.25}$$

where $\boldsymbol{\mathcal{L}}(t)$ is a path in the parameter space determined by the time-dependent vector-function $\boldsymbol{\mathcal{R}}(t)$.

The main purpose of Berry's consideration [1] was to give an analysis of the particular case of adiabatic changing, that is the cyclic change of parameters $\boldsymbol{\mathcal{R}}(t)$. For this purpose, we assume that the system was initially in one of the eigenstates $|u_n[\boldsymbol{\mathcal{R}}(0)]\rangle$. After some time T, the parameters return to their original values $\boldsymbol{\mathcal{R}}(T) = \boldsymbol{\mathcal{R}}(0)$. Hence, the Hamiltonian returns to the original form and the system return to the original state, but it acquires a phase

$$|\Psi[\boldsymbol{\mathcal{R}}(T)]\rangle = e^{-\frac{i}{\hbar}\int_0^t \varepsilon_n(t')dt' + i\gamma_n}|\Psi[\boldsymbol{\mathcal{R}}(0)]\rangle. \tag{1.26}$$

This phase is a sum of the usual dynamical phase, $-(1/\hbar)\int_0^t \varepsilon_n(t')dt'$ corresponding to the evolution of the system during the period of time T, and a geometric part, γ_n, well-known as the Berry phase [1, 59]

$$\gamma_n = i\oint_{\mathcal{L}} \langle u_n(\boldsymbol{\mathcal{R}})|\nabla_{\boldsymbol{\mathcal{R}}}|u_n(\boldsymbol{\mathcal{R}})\rangle d\boldsymbol{\mathcal{R}}, \tag{1.27}$$

where $\mathcal{L}$ is a closed path in the parameter space $\boldsymbol{\mathcal{R}}$.

One should keep in mind, that as far as the initial states might be determined only up to an arbitrary phase $|\tilde{u}_n(\boldsymbol{\mathcal{R}})\rangle \equiv \mathrm{e}^{i\Phi_n}|u_n(\boldsymbol{\mathcal{R}})\rangle$, and this arbitrary phase might be a function of parameters, $\Phi_n \equiv \Phi_n(\boldsymbol{\mathcal{R}})$, the evaluation of the circuit integral (1.27) for the state $|\tilde{u}_n(\boldsymbol{\mathcal{R}})\rangle \equiv \mathrm{e}^{i\Phi_n}|u_n(\boldsymbol{\mathcal{R}})\rangle$ might lead to an ambiguous result

$$\tilde{\gamma}_n(\boldsymbol{\mathcal{R}}) = \gamma_n + i \oint_{\mathcal{L}} \nabla_{\boldsymbol{\mathcal{R}}}\Phi_n(\boldsymbol{\mathcal{R}}) d\boldsymbol{\mathcal{R}}. \tag{1.28}$$

This ambiguity can be avoided by transforming the circuit integral (1.28) into the surface integral by means of the Stokes theorem [68]

$$\tilde{\gamma}_n(C) = \gamma_n(C) = -\mathrm{Im} \int\int_C \mathrm{d}\mathbf{S} \cdot \nabla_{\boldsymbol{\mathcal{R}}} \times \langle u_n(\boldsymbol{\mathcal{R}})|\nabla_{\boldsymbol{\mathcal{R}}} u_n(\boldsymbol{\mathcal{R}})\rangle \tag{1.29}$$

where the surface C is the surface spanned by the closed curve $\mathcal{L}$. We achieve this result

$$\mathrm{Im} \int\int_C \mathrm{d}\mathbf{S} \cdot \nabla_{\boldsymbol{\mathcal{R}}} \times \nabla_{\boldsymbol{\mathcal{R}}}\Phi_n(\boldsymbol{\mathcal{R}}) = 0, \tag{1.30}$$

because the equality $\mathrm{rot}\,\mathrm{grad}\,\Phi = 0$ holds for any function Φ. Therefore, the Berry phase is uniquely determined by the surface integral [1].

Moreover, Berry has shown that Eq. (1.29) can be expressed in terms of the "quasi"-magnetic field $\mathbf{V}_n(\boldsymbol{\mathcal{R}})$

$$\gamma_n(C) = -\int\int_C \mathrm{d}\mathbf{S} \cdot \mathbf{V}_n(\boldsymbol{\mathcal{R}}), \tag{1.31}$$

where

$$\mathbf{V}_n(\boldsymbol{\mathcal{R}}) \equiv \mathrm{Im} \sum_{m \neq n} \frac{\langle u_n(\boldsymbol{\mathcal{R}})|\nabla_{\boldsymbol{\mathcal{R}}}\hat{H}(\boldsymbol{\mathcal{R}})|u_m(\boldsymbol{\mathcal{R}})\rangle \times \langle u_m(\boldsymbol{\mathcal{R}})|\nabla_{\boldsymbol{\mathcal{R}}}\hat{H}(\boldsymbol{\mathcal{R}})|u_n(\boldsymbol{\mathcal{R}})\rangle}{[E_m(\boldsymbol{\mathcal{R}}) - E_n(\boldsymbol{\mathcal{R}})]^2}. \tag{1.32}$$

We would like to underline that the quantity $\mathbf{V}_n(\boldsymbol{\mathcal{R}})$ here is analogous to a magnetic field with vector potential $\mathrm{Im}\langle u_n(\boldsymbol{\mathcal{R}})|\nabla_{\boldsymbol{\mathcal{R}}} u_n(\boldsymbol{\mathcal{R}})\rangle$. Equations (1.31) and (1.32) reveal the truly geometric character of the Berry phase. One sees that this phase does not depend on time, but only on the circuit in the parameter space. Moreover, it does not depend on the velocity with which the circuit is traversed, as far as the change of parameters $\boldsymbol{\mathcal{R}}$ with time remains adiabatic.

The most important feature of the equation describing the "quasi"- magnetic field $\mathbf{V}_n(\boldsymbol{\mathcal{R}})$, Eq. (1.32), is the dependence on the difference of the two eigenenergies in the denominator, leading to the non-vanishing contributions into the sum only at the points $\boldsymbol{\mathcal{R}}_*$ of the so called "accidental" degeneracy,

$$E_m(\boldsymbol{\mathcal{R}}_*) = E_n(\boldsymbol{\mathcal{R}}_*), \tag{1.33}$$

that is the point in the parameter space at which two eigenenergies coincide for some particular parameter values. Hence, non-zero Berry phase occurs in the evolution of the systems, which have the degeneracy of the spectrum at certain point in the parameter space, called the degeneracy point $\boldsymbol{\mathcal{R}}_*$.

We will show an occurrence of the degeneracy points $\boldsymbol{\mathcal{R}}_*$ in the atomic spectra for the interaction of the atom with the laser field in Sec. 3.2.1.

Chapter 2

Atom-field interaction: a brief summary

In this chapter we briefly summarize the basic element of the coherent atom-field interaction [69], that is, spontaneous emission is not taken into account, and derive the Hamiltonian describing a two-level atom interacting with the laser field, which we treat classically.

2.1 The Hamiltonian of the atom-field interaction

First we introduce the concept of a two-level atom. Of course, any real atom has an infinite number of levels. However, when we shine monochromatic laser light on such an atom and the laser frequency is close to a particular transition frequency, then the probability of this transition is much larger than the probabilities of any other transition. In this particular case we can consider an atom as a two-level system. The two-level model is very useful and popular in quantum atom optics because it provides the detailed description of the atom-field interaction and allows one to obtain analytic solutions [70, 71].

Therefore, we describe the internal state of the atom by taking into account the energy eigenvalues for the ground $|g\rangle$ and the excited $|e\rangle$ levels, $E_g \equiv \hbar\omega_g$ and $E_e \equiv \hbar\omega_e$, respectively

$$\hat{H}_a|g\rangle = E_g|g\rangle, \quad \hat{H}_a|e\rangle = E_e|e\rangle. \tag{2.1}$$

The state of the atom $|\Psi\rangle$ is described by the superposition

$$|\Psi\rangle = \psi_g(\mathbf{r},t)\exp\left(-\frac{i}{\hbar}E_g t\right)|g\rangle + \psi_e(\mathbf{r},t)\exp\left(-\frac{i}{\hbar}E_e t\right)|e\rangle, \tag{2.2}$$

where we have introduced the probability amplitudes ψ_g and ψ_e of the ground and excited state population, respectively.

Next we use the dipole approximation, that is we neglect the spatial dependence of the field on the atom-length range [59, 69, 70, 72–75].

Moreover, we consider the coherent interaction where the spontaneous emission is not taken into account [69].

Thus, within these approximations, we describe the mechanical and the optical properties of the atom interacting with the electromagnetic field $\mathbf{E}(\mathbf{r},t)$ by the Schrödinger equation

$$\mathrm{i}\hbar\frac{\mathrm{d}}{\mathrm{d}t}|\Psi(t)\rangle = \left(\hat{H}_a - \mathbf{d}\cdot\mathbf{E}\right)|\Psi(t)\rangle. \tag{2.3}$$

Here $\hat{H}_a$ denotes the Hamiltonian of the free two-level atom.

Substituting an ansatz

$$|\Psi(t)\rangle = A_g(t;\mathbf{r})\mathrm{e}^{-\mathrm{i}\omega_g t}|g\rangle + A_e(t;\mathbf{r})\mathrm{e}^{-\mathrm{i}\omega_e t}|e\rangle \tag{2.4}$$

into the Schrödinger equation (2.3), we obtain

$$\mathrm{i}\hbar\frac{\partial A_e}{\partial t} = -\wp^*\cdot\mathbf{E}\,A_g\mathrm{e}^{\mathrm{i}(\omega_e-\omega_g)t} \tag{2.5}$$

$$\mathrm{i}\hbar\frac{\partial A_g}{\partial t} = -\wp\cdot\mathbf{E}\,A_e\mathrm{e}^{-\mathrm{i}(\omega_e-\omega_g)t} \tag{2.6}$$

where we have introduced the matrix element $\wp \equiv \langle g|\mathbf{d}|e\rangle$ of the atomic dipole moment operator [76]. The two-level approximation allows us to consider the dipole moment matrix element as a real-valued function

$$\wp \equiv \langle e|\hat{\mathbf{d}}|g\rangle = \langle g|\hat{\mathbf{d}}|e\rangle. \tag{2.7}$$

Substituting the explicit dependence

$$\mathbf{E}(\mathbf{r},t) = \mathbf{E}_0(\mathbf{r},t)\cos(\omega t) \tag{2.8}$$

of the light field on time and using the rotating wave approximation, that is we neglect the terms oscillating with twice the laser frequency, we obtain

$$\mathrm{i}\hbar\frac{\partial A_e}{\partial t} = -\frac{V_0}{2}A_g\mathrm{e}^{i\Delta t} \tag{2.9}$$

$$\mathrm{i}\hbar\frac{\partial A_g}{\partial t} = -\frac{V_0}{2}A_e\mathrm{e}^{-i\Delta t} \tag{2.10}$$

where the detuning $\Delta \equiv E_e - E_g - \omega \ll \omega$ and the operator $V_0 \equiv \wp\cdot\mathbf{E}_0$ are introduced.

In some particular cases of the atom-field interaction one can obtain an exact analytical solution of the system of equations defined by Eq. (2.9) and (2.10). One of these cases is presented in the next section.

2.2 Inverse cosh-envelope: exact solution

In the particular case of the time dependence

$$\mathbf{E}_0(t) = \mathcal{E}_0/\cosh(t/\tau) \tag{2.11}$$

one can solve the system Eq. (2.9) and (2.10) exactly, expressing the solution in terms of hypergeometric functions [69].

First we rewrite V_0 as $V_0 \equiv -\hbar\Omega_0/\cosh(t/\tau)$, where τ is the time of interaction, and Ω_0 denotes time-independent Rabi-frequency

$$\Omega_0 \equiv \frac{\wp \cdot \mathcal{E}_0}{\hbar}. \tag{2.12}$$

Then we express A_g in terms of $\dot{A}_e$ using Eq. (2.9)

$$A_g = \frac{2\mathrm{i}\cosh(t/\tau)}{\Omega_0}\dot{A}_e \mathrm{e}^{-i\Delta t}, \tag{2.13}$$

substitute this expression into Eq. (2.10) to obtain the second order differential equation

$$\ddot{A}_e + \dot{A}_e\left[\frac{1}{\tau}\tanh(t/\tau) - \mathrm{i}\Delta\right] + A_e\frac{\Omega_0^2}{4\cosh^2(t/\tau)} = 0. \tag{2.14}$$

for the $\dot{A}_e$. After substituting

$$z \equiv \frac{1}{2}\left[1 + \tanh(t/\tau)\right] \tag{2.15}$$

we receive the well-known hypergeometric equation [77]

$$z(1-z)\frac{\mathrm{d}^2 A_e}{\mathrm{d}z^2} + [c - (a+b+1)z]\frac{\mathrm{d}A_e}{\mathrm{d}z} - abA_e = 0 \tag{2.16}$$

with the parameters

$$a = -b \equiv |\Omega_0|\tau/2 \tag{2.17}$$

and

$$c \equiv \frac{1}{2}(1 - \mathrm{i}\Delta\tau). \tag{2.18}$$

The general solution of the hypergeometric equation Eq. (2.16) can be presented in the form of the linear combination of two independent solutions, hypergeometric functions $F(a,b;c;z)$ and $F(a-c+1, b-c+1; 2-c; z)$ [77], that is

$$A_e(z) = AF(a,b;c;z) + Bz^{1-c}F(a-c+1, b-c+1; 2-c; z), \tag{2.19}$$

where the constants A and B are determined by the initial conditions.

We assume an atom being initially in the ground state, which gives the initial conditions for the functions $A_e(t)$ and $A_g(t)$ are $A_e(t=-\infty) \equiv A_e(z=0) \equiv 0$ and $A_g(t=-\infty) \equiv A_g(z=0) \equiv 1$. Using these initial conditions we easily obtain $A \equiv 0$.

Moreover, we find B from the initial condition on the first derivative of the function $A_e(t)$, $\mathrm{d}A_e/\mathrm{d}z(z \to 0)$, using Eq.(2.9), which yields

$$B \equiv -\frac{ia}{1-c}. \tag{2.20}$$

Thus, we arrive at the expression for the probability amplitude of finding the atom in the excited state

$$A_e(z) \equiv -\frac{ia}{1-c} z^{1-c} F(a-c+1, b-c+1; 2-c; z). \tag{2.21}$$

Repeating the very same procedure with respect to the probability amplitude of finding the atom in the ground state A_g, we receive

$$A_g(z) \equiv F(a, b; c^*; z). \tag{2.22}$$

We find ourselves in the position of determining the amplitudes A_g and A_e at the limit $t \to \infty$, that is at the limit $z \to 1$.

Recalling the well-known relation [77]

$$F(a, b; c; 1) = \frac{\Gamma(c)\Gamma(c-a-b)}{\Gamma(c-a)\Gamma(c-b)} \tag{2.23}$$

for the hypergeometrical function of $z = 1$ and, using the properties of the Gamma-function $\Gamma(x)$, we derive

$$A_e(t \to \infty) = -i\frac{\sin(\pi a)}{\sin(\pi c)} \tag{2.24}$$

and

$$A_g(t \to \infty) = \frac{\Gamma^2(c^*)}{\Gamma(c^*-a)\Gamma(c^*+a)}. \tag{2.25}$$

Next we investigate the case of $\Delta\tau \gg 1$, which will turn out to be useful in Sec. 3.2. This condition allows us, see Eq. (2.18) to use the Stirling's formula [77]

$$\Gamma(x) \sim \mathrm{e}^{-x} x^{x-1/2} \sqrt{2\pi} \tag{2.26}$$

for $x \to \infty$ and $|\arg x| < \pi$. We rewrite the second equation of the system Eq. (2.24), Eq. (2.25) as

$$A_g(t \to \infty) = \exp\left\{2\ln\left[\Gamma(c^*)\right] - \ln\left[\Gamma(c^*-a)\right] - \ln\left[\Gamma(c^*+a)\right]\right\}. \tag{2.27}$$

With the help of the transformation formula [78]

$$\arctan(x) + \arctan(1/x) = \pm\frac{\pi}{2} \quad \begin{matrix} \mathrm{Re}\, x \geq 0 \\ \mathrm{Re}\, x < 0 \end{matrix} \tag{2.28}$$

we can cast Eq.(2.18) with the form

$$c^* \equiv \frac{1}{2}\sqrt{1+\Delta^2\tau^2}\exp\left\{\mathrm{i}\frac{\pi}{2}\mathrm{sgn}\Delta - \mathrm{i}\arctan\left(\frac{1}{\Delta\tau}\right)\right\}. \tag{2.29}$$

Finally we can use the Taylor expansion of the expression Eq. (2.27) for the probability amplitude of finding the atom in the ground state at infinitely long times $t \to \infty$ with respect to the infinitely small number $1/(\Delta\tau)$

$$f\left(x_0 + \frac{1}{\Delta\tau}\right) \sim f(x_0) + \frac{1}{\Delta\tau}\left.\frac{\mathrm{d}f}{\mathrm{d}x}\right|_{x=x_0}. \tag{2.30}$$

Neglecting higher order terms of the expansion, we arrive at

$$A_g(t\to\infty) = \exp\left(-\mathrm{i}\Delta\tau\ln\sqrt{1+\frac{|\Omega_0|^2}{\Delta^2}} + \mathrm{i}|\Omega_0|\tau\arctan\frac{|\Omega_0|}{\Delta}\right). \tag{2.31}$$

It is easy to show the vanishing of the probability amplitude $A_e(t \to \infty)$. While $\cosh(\infty) = \infty$, one immediately sees from the Eq. (2.24), Eq. (2.25) that $A_e(t \to \infty) \to 0$. This fact is purely due to the adiabaticity of the interaction, which assures that the atom does not make any transitions during the process of scattering by the standing wave field and remains in its initial state, which we have chosen to be the ground one by giving the initial conditions in the calculations above.

Chapter 3

Atom optics and Berry phase

In the previous chapters we have recalled the general concept of the Berry phase and the foundations of the atom-light interaction. In this chapter we consider the scattering of a two-level atom by a standing near-resonant electromagnetic wave and demonstrate the appearance of the Berry phase in this process.

3.1 Atomic scattering: standing wave

In the present section we formulate the problem of scattering of a two-level atom by two running electromagnetic waves with almost opposite wave vectors. For this purpose we first derive the Hamiltonian of the problem and then evaluate the matrix element of the interaction. We show that under appropriate conditions this quantity factorizes into a product of three terms, which allows us to imprint the center-of-mass motion onto a geometric phase.

3.1.1 Set-up

The near-resonant standing light field is created by two traveling waves of wave vectors $\mathbf{k}_1 \equiv \{k\cos\alpha, k\sin\alpha\}$ and $\mathbf{k}_2 \equiv \{-k\cos\alpha, k\sin\alpha\}$. Both fields form an angle α relative to the x-axis of a Cartesian coordinate system as shown in Fig. 3.1. The two running waves have identical wave number, that is $|\mathbf{k}_1| = |\mathbf{k}_2| \equiv k$, but propagate against each other since $(\mathbf{k}_1)_x = -(\mathbf{k}_2)_x$. As a result the electric field of the wave reads

$$\mathbf{E}(t,\mathbf{r}) = \mathbf{E}_0(\mathbf{r})[\sin(\mathbf{k}_2\cdot\mathbf{r}-\omega t) - \sin(\mathbf{k}_1\cdot\mathbf{r}-\omega t)], \tag{3.1}$$

where $\mathbf{E}_0(\mathbf{r})$ describes the position-dependent real-valued amplitude of the wave and ω is the frequency.

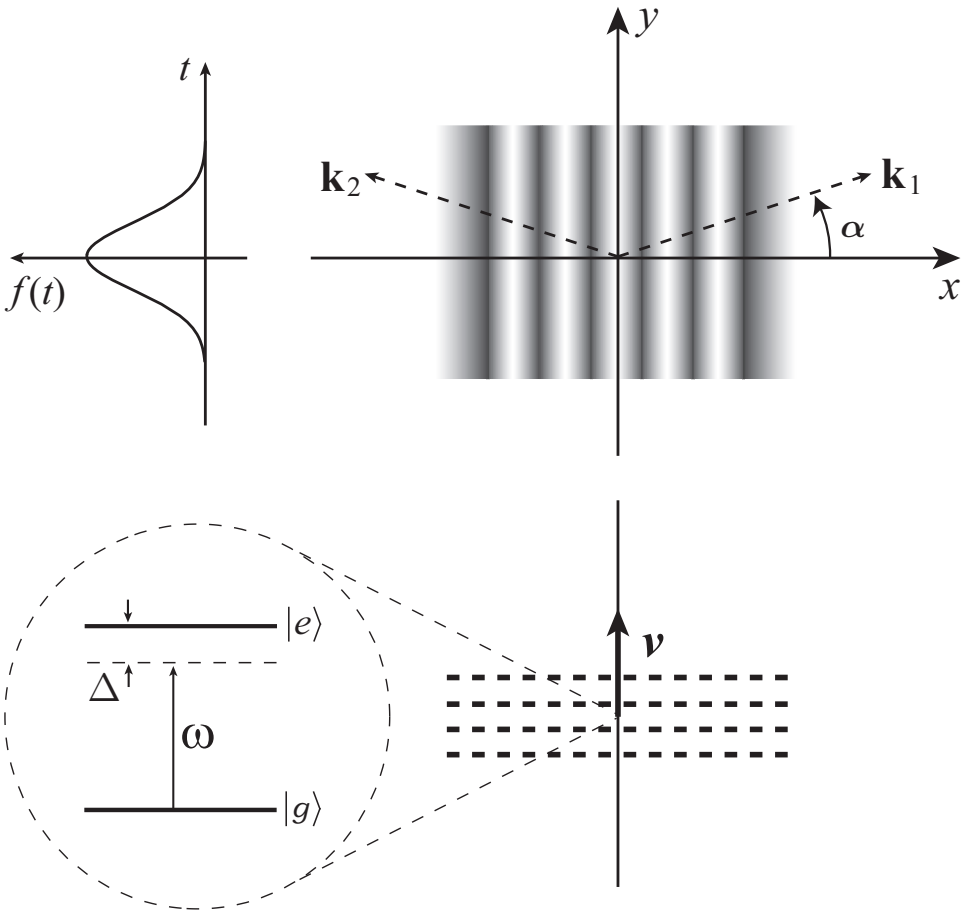


Figure 3.1: Scattering of a two-level atom by a standing electromagnetic field formed by two propagating waves of wave-vectors $\mathbf{k}_1$ and $\mathbf{k}_2$. These wave vectors $\mathbf{k}_1$ and $\mathbf{k}_2$ form an angle α and $\pi - \alpha$ with respect to the x-axis, respectively. The wave function of the atomic center-of-mass motion has a form of a plane wave. The envelope of the field along the y-axis translates into the time dependent function $f = f(t)$ as the atom propagates through the field with velocity $\mathbf{v} = v\,\mathbf{e}_y$. The frequency ω of the field is detuned from the atomic transition between the ground $|g\rangle$ and the excited $|e\rangle$ states by Δ.

The time evolution of the state-vector $|\Psi\rangle$ of the two-level atom interacting with the electromagnetic field follows from the Schrödinger equation [59, 69]

$$\mathrm{i}\hbar\frac{\mathrm{d}}{\mathrm{d}t}|\Psi(t)\rangle = \left(\hat{H}_{cm} + \hat{H}_a - \mathbf{d}\cdot\mathbf{E}\right)|\Psi(t)\rangle, \tag{3.2}$$

where the Hamiltonian

$$\hat{H}_{cm} \equiv \frac{\hat{\mathbf{p}}^2}{2M} \tag{3.3}$$

contains the operator of the kinetic energy of the center-of-mass motion of the atom of mass M. Moreover, $\hat{H}_a$ denotes the Hamiltonian of the free two-level atom with energy eigenstates $|e\rangle$ and $|g\rangle$ and energy eigenvalues $E_e \equiv \hbar\omega_e$ and $E_g \equiv \hbar\omega_g$ corresponding to the excited and the ground states, respectively, see Fig. 3.1. The interaction between the atom and the electromagnetic wave is described by the dipole operator $\mathbf{d}$.

The atom propagates along the y-axis with a macroscopic velocity v. For this reason we treat this motion classically that is we set $y = vt$. In contrast, the motion along the x-axis is described quantum mechanically. Therefore, we make the Raman-Nath approximation [59], that is we neglect the kinetic energy operator along the x-axis, Eq. (3.3), in the Schrödinger equation Eq. (3.2). Here we assume that the displacement of the atom along the x-axis during the time τ caused by its interaction with the standing light wave is small compared to its wave length. Indeed, the velocity acquired due to the resonant interaction of an atom with the standing light wave can be estimated as

$$\langle v_x\rangle \sim \frac{\hbar k}{M}\Omega\tau, \tag{3.4}$$

where Ω is the characteristic value of the Rabi frequency defined below. Hence, we obtain

$$\langle v_x\rangle\tau \ll 1/k \quad \text{or} \quad \omega_{rec}\tau^2\Omega \ll 1, \tag{3.5}$$

where

$$\omega_{rec} = \hbar k^2/(2M) \tag{3.6}$$

is the recoil frequency. Since the kinetic energy operator $\hat{\mathbf{p}}_x^2/(2M)$ is omitted in Eq. (3.2), the coordinate x is considered as a parameter.

The second approximation is in neglecting spontaneous emission due to the small interaction time τ of the atom with the field

$$\Gamma\tau w \leq 1. \tag{3.7}$$

Here Γ is the spontaneous emission rate of the excited level, w is the population of the excited level. In the case of exact resonance $\Delta = 0$ with the maximal value of the population probability of the excited level $w_m = 1/2$. In near resonance $|\Delta| \neq 0$, the maximal value of the probability to be in the excited level in the case of large

detuning $\hbar\Delta \gg |\langle e|\mathbf{d}\cdot\mathbf{E}|g\rangle|$ is $w_m = |\langle e|\mathbf{d}\cdot\mathbf{E}|g\rangle|^2/(2\hbar\Delta)^2$. Here we have introduced the detuning

$$\Delta \equiv \omega_e - \omega_g - \omega \tag{3.8}$$

between the frequencies of the atomic transition and the electromagnetic wave.

As a result we arrive at the Schrödinger equation

$$\mathrm{i}\hbar\frac{\mathrm{d}}{\mathrm{d}t}|\Psi(t)\rangle = \left(\hat{H}_a - \mathbf{d}\cdot\mathbf{E}\right)|\Psi(t)\rangle. \tag{3.9}$$

In order to solve this equation we make the ansatz

$$|\Psi(t)\rangle = A_g(t;\mathbf{r})\mathrm{e}^{-\mathrm{i}(\omega_g+\Delta/2)t}|g\rangle + A_e(t;\mathbf{r})\mathrm{e}^{-\mathrm{i}(\omega_e-\Delta/2)t}|e\rangle. \tag{3.10}$$

We emphasize that the amplitudes A_g and A_e depend on the time variable t, but only depend on the position vector $\mathbf{r}$ as a parameter.

When we substitute this ansatz (3.10) into the Schrödinger equation (3.9), we arrive at

$$\mathrm{i}\hbar\frac{\mathrm{d}}{\mathrm{d}t}\begin{pmatrix}A_e\\A_g\end{pmatrix} = \hat{H}\begin{pmatrix}A_e\\A_g\end{pmatrix}, \tag{3.11}$$

where the Hamiltonian

$$\hat{H} = \frac{1}{2}\begin{pmatrix}\hbar\Delta & V^*\\ V & -\hbar\Delta\end{pmatrix} \tag{3.12}$$

depends on the coupling matrix element

$$V(t;\mathbf{r}) \equiv -2e^{-\mathrm{i}\omega t}\langle g|\mathbf{d}\cdot\mathbf{E}(t,\mathbf{r})|e\rangle. \tag{3.13}$$

3.1.2 Explicit expression for interaction matrix element

The remaining task is to derive an explicit expression for the matrix element V defined by Eq. (3.13) in the presence of the two electric fields. For this purpose we express the sine functions in Eq. (3.1) as a sum of exponentials

$$\mathbf{E} = \frac{\mathbf{E}_0}{2\mathrm{i}}[(\mathrm{e}^{\mathrm{i}\mathbf{k}_2\cdot\mathbf{r}} - \mathrm{e}^{\mathrm{i}\mathbf{k}_1\cdot\mathbf{r}})\mathrm{e}^{-\mathrm{i}\omega t} - (\mathrm{e}^{-\mathrm{i}\mathbf{k}_2\cdot\mathbf{r}} - \mathrm{e}^{-\mathrm{i}\mathbf{k}_1\cdot\mathbf{r}})\mathrm{e}^{\mathrm{i}\omega t}] \tag{3.14}$$

and evaluate V neglecting terms oscillating with 2ω, that is we make the rotating wave approximation which yields

$$V(t;\mathbf{r}) \approx -\wp\cdot\mathbf{E}_0(\mathbf{r})\frac{1}{\mathrm{i}}(\mathrm{e}^{-\mathrm{i}\mathbf{k}_1\cdot\mathbf{r}} - \mathrm{e}^{-\mathrm{i}\mathbf{k}_2\cdot\mathbf{r}}). \tag{3.15}$$

Here we have introduced the dipole matrix element $\wp \equiv \langle g|\mathbf{d}|e\rangle$, which can be considered as real-valued in the case of the two-level atom.

Next we substitute the explicit form of the wave vectors $\mathbf{k}_1$ and $\mathbf{k}_2$ into Eq. (3.15) and find

$$V(t;\mathbf{r}) \approx 2\wp \cdot \mathbf{E}_0(\mathbf{r})\mathrm{e}^{-\mathrm{i}ky\sin\alpha}\sin(kx\cos\alpha). \tag{3.16}$$

At this point we make use of the fact that the motion of the atom along the y-axis is treated classically. As a result we can replace the y-coordinate by $y = vt$, where v is the velocity along the y-direction. The x-coordinate only appears as a parameter.

Moreover, we assume that the envelope $\mathbf{E}_0 = \mathbf{E}_0(\mathbf{r})$ of the electromagnetic wave is of the form

$$\mathbf{E}_0(\mathbf{r}) = \mathbf{E}_0(x, y). \tag{3.17}$$

When we now substitute $y = vt$, the coupling matrix element V given by Eq. (3.16) takes the form

$$V(t;\mathbf{r}) = \hbar\Omega(x,t)\mathrm{e}^{-\mathrm{i}\omega_\alpha t}, \tag{3.18}$$

where we have introduced the Doppler frequency

$$\omega_\alpha \equiv kv\sin\alpha \tag{3.19}$$

and the Rabi frequency

$$\Omega(x,t) \equiv \frac{2}{\hbar}\wp \cdot \mathbf{E}_0(x,vt)\sin(kx\cos\alpha). \tag{3.20}$$

For the sake of simplicity we assume that we can separate the x- and y-dependence of $\mathbf{E}_0$, that is

$$\mathbf{E}_0(x,vt) = \boldsymbol{\mathcal{E}}_0(x)f(t) \tag{3.21}$$

where $f = f(t)$ denotes the envelope function along the y-axis.

As a result Eq. (3.20) reduces to

$$\Omega(x,t) = \Omega(x)f(t) \tag{3.22}$$

where

$$\Omega(x) \equiv 2\frac{\wp \cdot \boldsymbol{\mathcal{E}}_0(x)}{\hbar}\sin(kx\cos\alpha) \tag{3.23}$$

denotes the position-dependent Rabi-frequency.

We conclude by substituting Eq. (3.22) into the expression Eq. (3.18) for V which yields

$$V(t;\mathbf{r}) = \hbar\Omega(x)f(t)\mathrm{e}^{-\mathrm{i}\omega_\alpha t}. \tag{3.24}$$

Hence, the coupling matrix element V consists of the product of three terms: (i) the position-dependent coupling energy $\hbar\Omega(x)$, (ii) the envelope function $f = f(t)$, and (iii) the time-dependent phase factor $\exp(-i\omega_\alpha t)$ due to the motion of the atom through the field.

3.2 Dynamical and geometric phases

In the present section we connect the Hamiltonian Eq. (3.12) together with the explicit expression for the matrix element V, Eq. (3.18), to the Hamiltonian used by Berry to derive the geometric phase [1]. This approach allows us to take advantage of the results derived in Ref. [1]. Moreover, we establish the connection between the dressed states and the atomic states.

3.2.1 Connection to Berry's formulation

For this purpose we make the identifications

$$X \equiv \mathrm{Re}\, V, \quad Y \equiv \mathrm{Im}\, V, \quad Z \equiv \hbar\Delta \tag{3.25}$$

and the Hamiltonian Eq. (3.12) takes the form considered by Berry [1].

$$H(\boldsymbol{\mathcal{R}}) = \frac{1}{2}\begin{pmatrix} Z & X - \mathrm{i}Y \\ X + \mathrm{i}Y & -Z \end{pmatrix}, \tag{3.26}$$

where the real-valued parameters X, Y and Z form the vector $\boldsymbol{\mathcal{R}}$.

This Hamiltonian leads to the eigenvalues $\varepsilon^{(\pm)} = \pm\varepsilon$ with

$$\varepsilon \equiv \frac{1}{2}\sqrt{X^2 + Y^2 + Z^2} = \frac{1}{2}\sqrt{(\hbar\Delta)^2 + |V|^2}. \tag{3.27}$$

and the corresponding eigenstates

$$|\Psi^{(\pm)}\rangle = \frac{1}{\sqrt{2\mathcal{R}(\mathcal{R} \pm Z)}}\begin{pmatrix} Z \pm \mathcal{R} \\ X + \mathrm{i}Y \end{pmatrix}. \tag{3.28}$$

depend on all three components of $\boldsymbol{\mathcal{R}}$. Here we have introduced the abbreviation $\mathcal{R} \equiv |\boldsymbol{\mathcal{R}}|$.

Recalling Eq. (1.33) we derive from Eq. (3.27) the degeneracy point

$$\boldsymbol{\mathcal{R}}_* = 0, \tag{3.29}$$

that is the point in the parameter space given by $\Delta = 0$ and $V = 0$.

Let us now return to the determination of the adiabaticity criterion. The condition for the adiabatic turn-on and -off of the interaction is that at any time t the rate of change of the light-field amplitude is much smaller than the spacing between the time-dependent quasienergy levels. Hence, the parameters of the system should satisfy the inequality

$$\left|\frac{\dot{V}}{V}\right| \ll |\varepsilon_+ - \varepsilon_-|. \tag{3.30}$$

When we recall the expression Eq. (3.24) for the coupling matrix element V, we obtain from Eq. (3.30)

$$\left|\frac{\dot{f}}{f} - i\omega_\alpha\right| \ll \sqrt{\Delta^2 + |\Omega|^2 f^2(t)}. \tag{3.31}$$

Assuming that at large t the function $f(t)$ decreases exponentially $f(t \to \pm\infty) \propto \exp(-|t|/\tau)$, we arrive at the adiabaticity criterion

$$|\Delta|\tau \gg \sqrt{1 + (\omega_\alpha \tau)^2}. \tag{3.32}$$

In the adiabatic limit defined by Eq. (3.32), we remain in the adiabatic states $|\Psi^{(\pm)}\rangle$ which accumulate phases in the course of time.

When the time dependence of $\boldsymbol{\mathcal{R}}$ is such that $\boldsymbol{\mathcal{R}}$ returns at time $t = +T$ to its initial value $\boldsymbol{\mathcal{R}}(-T)$ the two instantaneous eigenstates $|\Psi^{(\pm)}\rangle$ acquire [1] the dynamical phases φ_D as well as the geometric phases φ_B with

$$\varphi_D \equiv \frac{1}{\hbar}\int_{-T}^{+T} \varepsilon(t)\mathrm{d}t \tag{3.33}$$

and

$$\varphi_B \equiv \int\int_{C(2T)} d\mathbf{S} \cdot \frac{\boldsymbol{\mathcal{R}}}{2\mathcal{R}^3} \tag{3.34}$$

where $C(2T)$ defines the surface of integration, i.e. the curve C develops to a closed circuit $C(2T)$ during the one cycle of parameter change given by the time $2T$ from $t = -T$ to $t = +T$.

As a result the eigenstates after a cyclic change read

$$|\Psi^{(\pm)}(+T)\rangle = \exp(\mp \mathrm{i}\varphi_D)\exp(\mp \mathrm{i}\varphi_B)|\Psi^{(\pm)}(-T)\rangle. \tag{3.35}$$

The geometric phase is solely determined by the flux $\boldsymbol{\mathcal{R}}/2\mathcal{R}^3$ through the area enclosed by the parameter $\boldsymbol{\mathcal{R}} = \boldsymbol{\mathcal{R}}(t)$ during one period of the parameter change, time interval $2T$.

3.2.2 Connection between dressed states and atomic states

The dynamical as well as the geometric phase are formulated in terms of dressed states which arise due to the interaction of the atom with the electromagnetic field. However, before the atom enters the field it is prepared in a well-defined internal state. For this reason we need to connect the dressed states $|\Psi^{(\pm)}\rangle$ and the atomic states $|g\rangle$ and $|e\rangle$.

Before the atom enters the light field, that is at the time $t = -T$, the interaction V vanishes, leading to $X = Y = 0$ and $\mathcal{R} = |Z| = \hbar|\Delta|$. Here we have assumed for the

sake of simplicity that the envelope function is a mesa function with a sharp turn-on at $-T$ and a sharp turn-off at T. Needless to say this assumption is not necessary and we will consider later a smooth envelope function.

Due to the appearance of the absolute value $|\Delta|$ of the detuning it is useful to consider the two cases of $\Delta < 0$ and $0 < \Delta$. Indeed, for $\Delta < 0$ we find

$$|\Psi^{(+)}(-T)\rangle = |g\rangle \quad \text{and} \quad |\Psi^{(-)}(-T)\rangle = -|e\rangle \tag{3.36}$$

whereas for $0 < \Delta$ we arrive at

$$|\Psi^{(+)}(-T)\rangle = |e\rangle \quad \text{and} \quad |\Psi^{(-)}(-T)\rangle = |g\rangle. \tag{3.37}$$

Hence, in the case of $\Delta < 0$ the ground and the excited states follow $|\Psi^{(+)}\rangle$ and $|\Psi^{(-)}\rangle$, respectively. For $0 < \Delta$ the ground state follows $|\Psi^{(-)}\rangle$ and the excited state follows $|\Psi^{(+)}\rangle$.

When we recall from Eq. (3.10) the prefactors $\exp[-\mathrm{i}(\omega_g \pm \Delta/2)t]$, we obtain that during the time $2T$ the ground state exponential prefactor gives a contribution into the ground state phase equal to $-\Delta T$. Summing it up with the dynamical part acquired due to the atom-field interaction Eq. (3.33), we pick up the total dynamical phase of the ground state

$$\beta \equiv \varphi_D - |\Delta|T. \tag{3.38}$$

Therefore, the total phase acquired by the ground state during interaction Eq. (3.10) is given by

$$\varphi_g \equiv \beta \mathrm{sgn}\Delta + \gamma, \tag{3.39}$$

where we have introduced from Eq. (3.34) the total Berry phase

$$\gamma = \varphi_B \mathrm{sgn}\Delta, \tag{3.40}$$

which finally does not depend on the sign of the detuning as we show in the following sections.

We choose the above definition of β and γ on purpose to underline the $\mathrm{sgn}\Delta$ dependence of the dynamical contribution, the benefit of which we use in Sec. 3.5.

The same procedure makes a contribution

$$\varphi_e \equiv -\varphi_g - \frac{\pi}{2}(1 - \mathrm{sgn}\Delta) \tag{3.41}$$

for the evolution of the excited state.

Note, that we have neglected the phase contributions proportional to ω_g and ω_e in Eq. (3.10). Indeed, we are interested only in interference experiments, where we split the atomic beam and let one part propagate freely and the other part be scattered by the standing wave. As the phase contributing terms proportional to ω_g and ω_e are the same for both parts, they will not contribute to the relative phase between these two parts and, hence, will not be observed in the experiment.

3.3 Circuit in parameter space

In Sec. 3.1.2 we have derived the explicit expression Eq. (3.24) for the interaction matrix element V of the coupling between the two atomic states. We are now in the position to discuss the path in parameter space traversed by $\boldsymbol{\mathcal{R}} = \boldsymbol{\mathcal{R}}(t)$ in the course of time. This path is defined by Eq. (3.25) together with the formula Eq. (3.24) for V.

Since according to Eq. (3.25) the Z-component of $\boldsymbol{\mathcal{R}}$ is given by the constant detuning Δ the circuit lies parallel to the XY-plane. Moreover, the path is given by

$$X(t;x) = \hbar|\Omega(x)|f(t)\cos(\omega_\alpha t) \tag{3.42}$$

and

$$Y(t;x) = -\hbar|\Omega(x)|f(t)\sin(\omega_\alpha t) \tag{3.43}$$

where we have recalled Eq. (3.24). Due to the position-dependence of Ω the circuit depends on x as a parameter.

The curve defined by Eqs. (3.42) and (3.43) is most conveniently described by the polar coordinates

$$\rho \equiv \hbar|\Omega|f \tag{3.44}$$

and

$$\phi \equiv \omega_\alpha t. \tag{3.45}$$

In these coordinates the circuit is given by the curve

$$\rho = \rho(\phi) = \hbar|\Omega|f(\phi/\omega_\alpha). \tag{3.46}$$

In Fig. 3.2 we illustrate circuits in parameter space for three examples of envelopes. All of them are symmetric in time, that is they satisfy the relation

$$f(-t) = f(t). \tag{3.47}$$

Moreover, we have chosen identical values for the maximum height of f in all three examples.

For the rectangular envelope

$$f_M \equiv \begin{cases} 1 & \text{for} \quad -\tau/2 < t < \tau/2 \\ 0 & \text{otherwise} \end{cases}, \tag{3.48}$$

of interaction time τ indicated in Fig. 3.2 by a dashed line, the circuit is a complete circle provided $\omega_\alpha \tau = 2\pi$.

In the case of the envelope

$$f_C(t) \equiv \begin{cases} \cos^2(\pi t/\tau) & \text{for} \quad -\tau/2 < t < \tau/2 \\ 0 & \text{otherwise} \end{cases}, \tag{3.49}$$

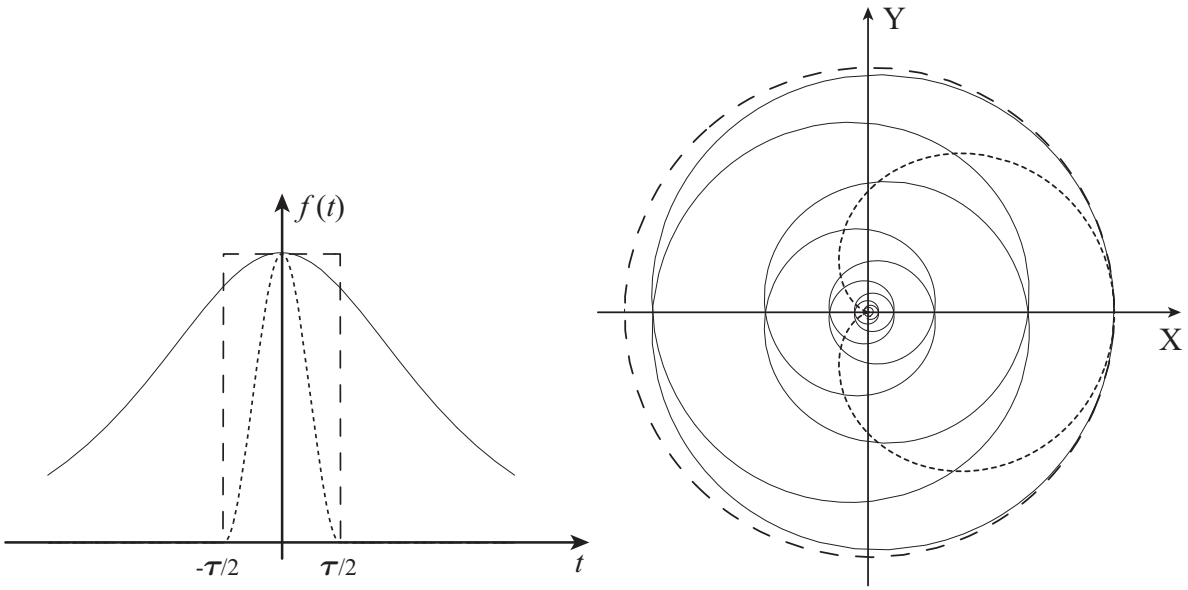


Figure 3.2: Translation of the envelope $f = f(t)$ of the electromagnetic field (left) into a circuit in parameter space (right) illustrated here for the three characteristic envelopes of a mesa function (dashed line), the squared-cos-potential (dotted line) and the Eckart potential (solid line). Whereas the mesa function gives rise to a circle (dashed line), the squared-cos-potential results in cardioid (dotted line), which we traverse only once provided the interaction time τ and the frequency ω_α satisfy the condition $\omega_\alpha \tau = 2\pi$. However, the Eckart envelope leads to an infinite amount of windings around the origin of parameter space.

in the shape of a squared cosine we find a cardioid as indicated by the dotted line. Again the curve is closed only provided $\omega_\alpha \tau = 2\pi$. The cardioid is aligned in the two-dimensional parameter space along the X-axis as shown in Fig. 3.2.

The model most relevant for the experimental realization is given by Eckart envelope

$$f_E(t) \equiv \cosh^{-1}(t/\tau). \tag{3.50}$$

We note from Eq. (3.44) that for $t = \pm\infty$ the amplitude ρ vanishes. Hence, the circuit initiates and terminates at the origin. In the course of time the amplitude ρ first increases and then decreases again. At the same time the angle ϕ increases monotonously. As a result the curve defining the circuit of $\boldsymbol{\mathcal{R}}$ circumvents the origin infinitely many times before it returns to it. However, due to the increase and decrease of ρ not all windings will be visible. The number of the prominent circuits is determined by the value of $\omega_\alpha \tau$. In Fig. 3.2 we have chosen $\omega_\alpha \tau = 2\pi$

The trajectory crosses itself infinitely many times. Due to the symmetry relation Eq. (3.47) these crossings take place on the X axis, as shown by the solid curve in Fig. 3.2. This property follows immediately from the condition $X(-t;x) = X(t;x)$ and $Y(-t;x) = Y(t;x)$, which with help of Eqs. (3.42) and (3.43) translates into the requirements

$$\cos(-\omega_\alpha t_m) = \cos(\omega_\alpha t_m) \tag{3.51}$$

and

$$\sin(-\omega_\alpha t_m) = \sin(\omega_\alpha t_m). \tag{3.52}$$

They are satisfied for

$$\omega_\alpha t_m = m\pi \tag{3.53}$$

where $m = 0, \pm 1, \pm 2...$

Indeed, when we substitute these times into the coordinates of the crossings we find $X_m = (-1)^m \hbar |\Omega(x, t_m)|$ and $Y_m = 0$.

3.4 Explicit expressions for phases

In the preceding section we have discussed the form of the circuits in parameter space for three examples of the longitudinal mode function of the electromagnetic field. In the present section we obtain explicit formula for the geometric phase, as well as the dynamical one.

3.4.1 Geometric phase

We start our analysis with the evaluation of the geometric phase. According to Eq. (3.34) we have to calculate the flux $\boldsymbol{\mathcal{R}}/(2\mathcal{R}^3)$ through the area enclosed by the circuit

in parameter space. Since the vector normal to this surface is along the Z-axis of the Cartesian coordinate system we find

$$\boldsymbol{\mathcal{R}} \cdot \mathrm{d}\mathbf{S} = -\hbar\Delta \mathrm{d}S, \tag{3.54}$$

and Eqs. (3.34) and (3.40) reduce to

$$\gamma = -\frac{1}{2}\hbar|\Delta| \int \mathrm{d}X \int \mathrm{d}Y \frac{1}{(X^2+Y^2+(\hbar\Delta)^2)^{3/2}}. \tag{3.55}$$

When we express this integral in the polar coordinates ρ and ϕ, defined by Eqs. (3.44) and (3.45), we arrive at

$$\gamma = -\frac{1}{2}\hbar|\Delta| \int_{\phi_i}^{\phi_f} \mathrm{d}\phi \int_0^{\rho(\phi)} \frac{\rho\,\mathrm{d}\rho}{(\rho^2+\hbar^2\Delta^2)^{3/2}}. \tag{3.56}$$

Here the upper limit $\rho = \rho(\phi)$ of the radial integral depends on the circuit in parameter space parametrized by the angle ϕ. The integration over ϕ runs between the initial and final angles of the curve, ϕ_i and ϕ_f, respectively. Their precise form is dictated by the shape of the circuit.

Integration over ρ yields

$$\gamma(x) = \frac{1}{2} \int_{\phi_i}^{\phi_f} \mathrm{d}\phi \left(\frac{1}{\sqrt{1+(\rho(\phi)/\hbar\Delta)^2}} - 1 \right), \tag{3.57}$$

which with the help of Eq. (3.46) leads us to the expression

$$\gamma = \frac{1}{2} \int_{\phi_i}^{\phi_f} \mathrm{d}\phi \left[\frac{1}{\sqrt{1+a^2(x)f^2(\phi/\omega_\alpha)}} - 1 \right] \tag{3.58}$$

for the geometric phase. Here we have introduced the dimensionless

$$a(x) \equiv \frac{|\Omega(x)|}{|\Delta|} \tag{3.59}$$

Rabi frequency.

The position-dependence of the geometric phase arises from the position-dependence of $a = a(x)$. Next we illustrate the influence of the shape of the circuit on this integration using the three envelope functions given by Eqs. (3.48), (3.49) and (3.50).

We show in Ch. 4.1 that the same result can be obtained within the WKB approach.

Mesa envelope

The mesa envelope f_M given by Eq. (3.48) is non-vanishing and constant only for the time interval $-\tau/2 < t < \tau/2$ and the expression Eq. (3.57) for the geometric phase reduces to

$$\gamma_M(x) = \frac{1}{2}\left(\frac{1}{\sqrt{1+a^2(x)}} - 1\right)(\phi_f - \phi_i). \tag{3.60}$$

From the definition Eq. (3.45) of the angle ϕ, together with the initial and end points, $-\tau/2$ and $\tau/2$, respectively, for the mesa envelope, we find

$$\phi_f - \phi_i = \omega_\alpha \tau. \tag{3.61}$$

However, we recall from Sec. 3.3 that the circuit is only closed provided $\omega_\alpha \tau = 2\pi$. As a result we obtain the final expression

$$\gamma_M(x) = \pi\left(\frac{1}{\sqrt{1+a^2(x)}} - 1\right) \tag{3.62}$$

for the geometric phase in the case of the mesa envelope.

In the case of the weak atom-laser interaction we satisfy the condition $a(x) \ll 1$. In this limit Eq. (3.62) reduces to

$$\gamma_M(x) = \sigma_M a^2(x)\pi, \tag{3.63}$$

where we have used the abbreviation $\sigma_M \equiv -1/2$.

The geometric phase is determined by the product of three terms: a numerical factor, the square of the dimensionless Rabi frequency, and π.

Squared-cos potential

We now turn to the envelope of the form of the squared-cosine potential given by Eq. (3.49). In this case the circuit in parameter space is a cardioid and the integral Eq. (3.58) determining the geometric phase takes the form

$$\gamma_C = \frac{1}{2}\int_{\phi_i}^{\phi_f} \mathrm{d}\phi \left(\frac{1}{\sqrt{1+a^2(x)\cos^4(\phi\pi/(\omega_\alpha\tau))}} - 1\right). \tag{3.64}$$

When we recall that the cardioid is closed only for $\omega_\alpha\tau = 2\pi$ the geometric phase Eq. (3.64) takes the form

$$\gamma_C = \frac{1}{2}\int_0^{2\pi} \mathrm{d}\phi \left(\frac{1}{\sqrt{1+a^2\cos^4(\phi/2)}} - 1\right), \tag{3.65}$$

where we have set $\phi_i = 0$ and $\phi_f = 2\pi$.

As a result we arrive at

$$\gamma_C = 2I_C - \pi, \tag{3.66}$$

where we have defined the integral

$$I_C \equiv \int_0^{\pi/2} \mathrm{d}\theta \frac{1}{\sqrt{1 + a^2 \cos^4\theta}}. \tag{3.67}$$

When we make the substitution

$$\cos\zeta \equiv \frac{\sqrt{1+a^2} - \tan^2\theta}{\sqrt{1+a^2} + \tan^2\theta} \tag{3.68}$$

we find

$$I_C \equiv \frac{1}{(a^2+1)^{1/4}} \mathrm{K}(\xi), \tag{3.69}$$

where we have recalled [79] the complete elliptical integral of the first kind,

$$\mathrm{K}(\xi) \equiv \int_0^{\pi/2} \mathrm{d}x \frac{1}{\sqrt{1 - \xi^2 \sin^2 x}} \tag{3.70}$$

with the parameter

$$\xi \equiv \frac{1}{\sqrt{2}} \sqrt{1 - \frac{1}{\sqrt{a^2+1}}}. \tag{3.71}$$

As a result, we arrive at the expression

$$\gamma_C = \frac{2}{(a^2+1)^{1/4}} \mathrm{K}\left(\frac{1}{\sqrt{2}} \sqrt{1 - \frac{1}{\sqrt{a^2+1}}} \right) - \pi \tag{3.72}$$

for the geometric phase in the case of the squared-cosine envelope.

For $|\xi|^2 \ll 1$ we recall [78] the asymptotic expansion

$$\mathrm{K}(\xi) = \frac{\pi}{2} \left[1 + \left(\frac{1}{2}\right)^2 \xi^2 + \left(\frac{1 \cdot 3}{2 \cdot 4}\right)^2 \xi^4 + ... \right] \tag{3.73}$$

which due to $a(x) \ll 1$ gives

$$\gamma_C(x) = \sigma_C a^2(x) \pi, \tag{3.74}$$

where we have introduced $\sigma_C \equiv -3/16$.

A comparison with the geometric phase Eq. (3.63) induced by the mesa envelope shows that the squared-cosine envelope has only resulted in a change of the numerical prefactor. We show in the further subsection 3.4.3 that this quadratic dependence of the geometric phase on the dimensionless Rabi frequency, $\gamma \propto a^2$ (for $a \ll 1$), occurs for any envelope form.

Eckart envelope

Next we turn to the Eckart envelope. Here the curve in parameter space circles around the origin infinitely many times. As a result we have $\phi_i = -\infty$ and $\phi_f = +\infty$ and Eq. (3.58) takes the form

$$\gamma_E = \frac{1}{2}\int_{-\infty}^{+\infty} \mathrm{d}\phi \left(\frac{1}{\sqrt{1 + a^2(x)\cosh^{-2}(\phi/(\omega_\alpha \tau))}} - 1 \right). \tag{3.75}$$

When we introduce the integration variable $\theta \equiv \phi/(\omega_\alpha \tau)$ and take into account the symmetry of the integrand we arrive at

$$\gamma_E = \omega_\alpha \tau I_E, \tag{3.76}$$

where we have introduced the integral

$$I_E \equiv \int_0^{\infty} \mathrm{d}\theta \left[\frac{\cosh\theta}{\sqrt{\cosh^2\theta + a^2}} - 1 \right]. \tag{3.77}$$

Next we recall the integral relation [80]

$$\int \mathrm{d}\theta \frac{\cosh\theta}{\sqrt{\cosh^2\theta + a^2}} = \ln(\sinh\theta + \sqrt{\cosh^2\theta + a^2}) \tag{3.78}$$

and find

$$I_E = \lim_{\theta\to\infty} \left\{ \ln\left[\frac{\sinh\theta + \sqrt{\cosh^2\theta + a^2}}{\sqrt{1 + a^2}} \right] - \theta \right\}, \tag{3.79}$$

which with the help of the asymptotic behavior

$$\sinh\theta \cong \cosh\theta \cong \frac{1}{2}\mathrm{e}^{\theta} \tag{3.80}$$

in the limit of $\theta \to \infty$ reduces to

$$I_E = -\frac{1}{2}\ln(1 + a^2). \tag{3.81}$$

We substitute this result into the expression Eq. (3.75) for γ_E and arrive at

$$\gamma_E(x) = -\pi \ln[1 + a^2(x)], \tag{3.82}$$

where we use the condition $\omega_\alpha \tau = 2\pi$ for having a closed circuit in parameter space.

In the weak-field limit $a(x) \ll 1$ we obtain from Eq. (3.82)

$$\gamma_E(x) = \sigma_E a^2(x)\pi \tag{3.83}$$

with the numerical factor $\sigma_E \equiv -1$.

We conclude by noting that we can rederive Eq. (3.82) by decomposing the path in the parameter space into a sequence of closed circuits and calculate the sum of the fluxes through each of these areas, as shown in Appendix A.

3.4.2 Dynamical phase

Next we turn to the dynamical phase. For this purpose we substitute the expression for V, Eq. (3.24), into the one for the quasi-energy ε, Eq. (3.27), and find

$$\varepsilon(t) = \frac{\hbar}{2}\sqrt{\Delta^2 + |\Omega(x)|^2 f^2(t)}. \tag{3.84}$$

When we substitute this expression into the Eq. (3.38) providing the total dynamical phase we arrive at

$$\beta = \frac{1}{2}\int_{-T}^{+T} \mathrm{d}t \left(\sqrt{\Delta^2 + |\Omega(x)|^2 f^2(t)} - |\Delta|\right). \tag{3.85}$$

Using the symmetry of the integrand we find

$$\beta = |\Delta| \int_{0}^{+T} \mathrm{d}t \left(\sqrt{1 + a^2 f^2(t)} - 1\right). \tag{3.86}$$

Now we are in the position to present the dynamical phase in the case of the different envelopes $f(t)$, Eq. (3.48), Eq. (3.49) and Eq. (3.50).

Mesa envelope

We start our analysis of the dynamical phase by substituting the expression for the rectangular envelope Eq. (3.48) into the general expression Eq. (3.86) for the dynamical phase

$$\beta_M = |\Delta| \int_{0}^{\tau/2} \mathrm{d}t \left(\sqrt{1 + a^2} - 1\right) = \frac{|\Delta|\tau}{2}\left(\sqrt{1 + a^2} - 1\right) \tag{3.87}$$

and obtain the expression

$$\beta_M = \frac{\pi|\Delta|}{\omega_\alpha}\left(\sqrt{1 + a^2} - 1\right), \tag{3.88}$$

where we have used the condition $\omega_\alpha \tau = 2\pi$. In the weak-field limit $a^2 \ll 1$ we arrive at

$$\beta_M = \frac{\pi|\Delta|}{2\omega_\alpha} a^2. \tag{3.89}$$

Recalling the expression, Eq. (3.63), for the geometric phase in the case of the rectangular envelope, we find

$$|\gamma_M/\beta_M| = |\omega_\alpha|/|\Delta|. \tag{3.90}$$

Squared-cos potential

Next we turn to the dynamical phase, Eq. (3.86), acquired during the interaction with the field of squared-cos envelope, Eq. (3.49),

$$\beta_C = |\Delta| \int_0^{\tau/2} \mathrm{d}t \left(\sqrt{1 + a^2 \cos^4(\pi t/\tau)} - 1 \right). \tag{3.91}$$

The integration of Eq. (3.91) gives the combination of the complete elliptic integrals of the first, second and third kind. For the sake of simplicity, we show the result already in the weak-field limit $a^2 \ll 1$ where it reads

$$\beta_C = \frac{3\pi|\Delta|}{16\omega_\alpha} a^2, \tag{3.92}$$

here we have used the condition $\omega_\alpha \tau = 2\pi$. Recalling the expression, Eq. (3.74), for the geometric phase in the case of the squared-cosine potential, we find the ratio

$$|\gamma_C/\beta_C| = |\omega_\alpha|/|\Delta| \tag{3.93}$$

the ratio of the geometric to the dynamical phase in the case of the squared-cos envelope.

Eckart envelope

In the case of the Eckart potential the field switches on and off according to the inverse of the cosh-function. Therefore, we can extend the limits $-T$ and $+T$ of the integration to $-\infty$ and $+\infty$, respectively. Hence, we find

$$\beta_E = |\Delta| \int_0^{+\infty} \mathrm{d}t \left(\sqrt{1 + a^2 \cosh^{-2}(t/\tau)} - 1 \right). \tag{3.94}$$

Making substitution

$$\sin\eta = \sqrt{\frac{a^2}{1+a^2}} \tan(t/\tau) \tag{3.95}$$

gives

$$\beta_E = |\Delta|\tau a \left[\arctan(a) - \int_0^{\arctan(a)} \mathrm{d}\eta \frac{1}{1 + \sqrt{1+a^2}\cos\eta} \right]. \tag{3.96}$$

When we recall [79] the integral relation

$$\int \mathrm{d}x \frac{1}{c + d\cos x} = \frac{1}{\sqrt{d^2 - c^2}} \ln \left[\frac{\sqrt{d^2 - c^2}\tan(x/2) + c + d}{\sqrt{d^2 - c^2}\tan(x/2) - c - d} \right] \tag{3.97}$$

for $c^2 < d^2$, and use the condition $\omega_\alpha \tau = 2\pi$ we arrive at

$$\beta_E = \frac{2\pi|\Delta|}{\omega_\alpha}\left[a \arctan a - \ln\sqrt{1+a^2})\right]. \tag{3.98}$$

For $a^2 \ll 1$ this expression transforms to

$$\beta_E = \frac{\pi|\Delta|}{\omega_\alpha}a^2. \tag{3.99}$$

Again after recalling Eq. (3.83), for the geometric phase in the case of the Eckart envelope, we find

$$|\gamma_E/\beta_E| = |\omega_\alpha|/|\Delta|. \tag{3.100}$$

3.4.3 Ratio γ/β in possible experiment

In the preceding sections we have shown that the absolute value of the ratio of the geometric phase to dynamical phase in the weak-field limit is given by the ratio $|\omega_\alpha/\Delta|$ independent of the details of the potential. We have shown this feature for the mesa, the squared-cosine and the Eckart potential. Now we generalize this result to any envelope $f(t)$ that satisfies the condition $a \ll 1$. Indeed, in the limit of a weak interaction, $a \ll 1$, the dynamical phase reads

$$\beta = \frac{\Delta}{2}\int_{-T}^{T} dt\left(\sqrt{1+a^2 f^2(t)} - 1\right) \approx \frac{\Delta a^2}{4}\int_{-T}^{T} dt\, f^2(t) \tag{3.101}$$

while the geometric phase is given by

$$\gamma = \frac{\omega_\alpha}{2}\int_{-T}^{T} dt\left[\frac{1}{\sqrt{1+a^2(x)f^2(t)}} - 1\right] \approx -\frac{\omega_\alpha a^2}{4}\int_{-T}^{T} dt\, f^2(t). \tag{3.102}$$

A comparison of the two expression reveals that in the limit of a weak field with $|\Omega| \ll |\Delta|$ the ratio between the geometric and dynamical phase reads

$$\left|\frac{\gamma}{\beta}\right| = \left|\frac{\omega_\alpha}{\Delta}\right| \tag{3.103}$$

and is determined only by the ratio ω_α to Δ. It is independent of the field envelope.

It is useful to estimate this ratio for typical experimental values. For instance, in the case of the $1s_5(J=2) \to 2p_3(J=3)$ transition in argon [25], and the wave length $\lambda = 812\text{nm}$, the resonance detuning $\Delta \simeq 3{\cdot}10^7\text{s}^{-1}$, the recoil frequency $\omega_{rec} \simeq 5{\cdot}10^4\text{s}^{-1}$, the velocity $v_y = 700$ m/s and the angle $\alpha = 10^{-4}$, we obtain from Eq. (3.103) the estimate

$$\left|\frac{\gamma}{\beta}\right| \simeq 0.1, \tag{3.104}$$

which is already feasible in a possible experiment.

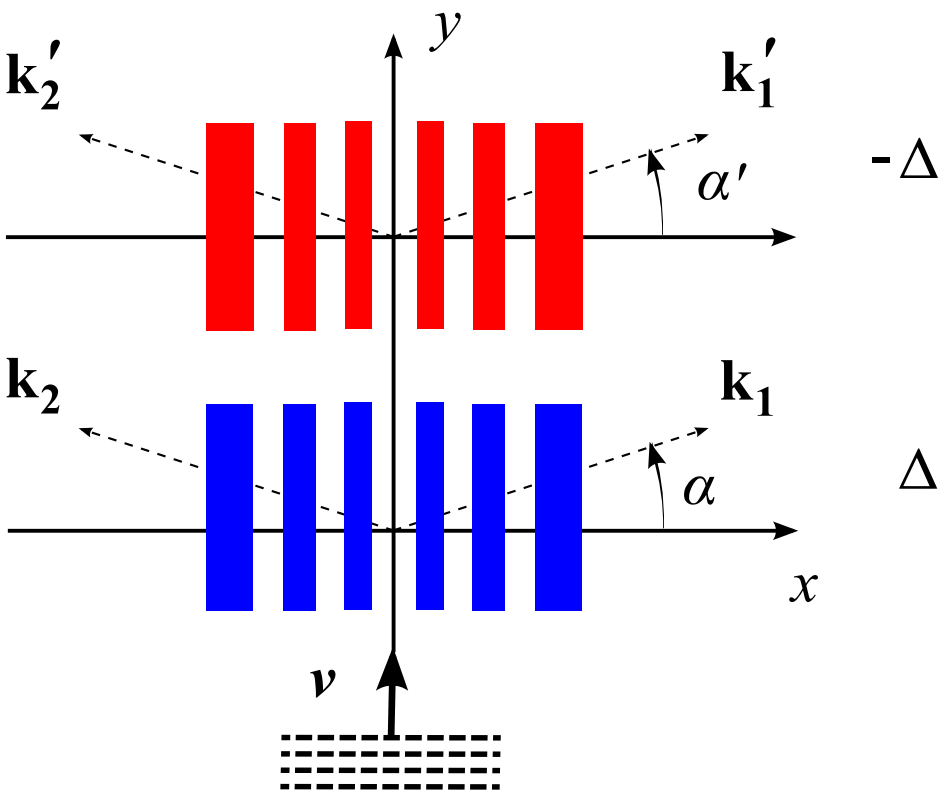


Figure 3.3: Cancellation of the dynamical phase by the consecutive scattering of a two-level atom by two standing waves: (i) blue-detuned, (ii) red-detuned.

3.5 Cancellation of the dynamical phase

Now we are in the position to analyze the results obtained in the previous chapters and propose a scheme for the dynamical phase cancellation. This cancellation is very important because of the detection intricacy of the Berry phase effect in the presence of the dynamical phase. The last one is always dominating. Moreover, due to its dependence on the systems energy, the dynamical phase is particularly sensitive to noise and easily disturbed by the slightest change of the system parameters. Now let us remind of the structure of the expressions for the total phases acquired by the ground and excited states, Eq. (3.39) and Eq. (3.41), respectively. Resuming the expressions for the total dynamical phase, Eq. (3.38), and geometric phase, Eq. (3.40), we see that the total phase of the states depends on the sign of the detuning in the dynamical part, but only on the absolute value in the geometric part, $\varphi_g = \beta \mathrm{sgn}\Delta + \gamma$. This fact allows us to suggest the simple intuitive scheme of the dynamical phase cancellation, as shown by Fig. 3.3. Indeed, since the dynamical part depends on the sign of the detuning, we propose to use two consecutive interactions of the atom with the standing waves, that

is, firstly with the blue detuned waves ($\Delta > 0$), secondly with the red detuned waves ($\Delta' = -\Delta < 0$). Hence, due to the opposite signs of the detuning, the dynamical contributions cancel each other if the condition $k\cos\alpha = k'\cos\alpha'$ is fulfilled, see Eq. (3.16). Here we introduced the dashed variables to describe the second standing wave. The geometric phase is summed up after the second scattering

$$\varphi_g^{(tot)} \equiv \varphi_g + \varphi_g' = \gamma + \gamma' \simeq 2\gamma. \tag{3.105}$$

Thus, in the proposed above configuration of the two consecutive scatterings of the atom by the opposite detuned standing waves, we receive cancellation of the dynamical phase and approximate doubling of the Berry phase. Of course, the time interval between two interactions of atom with standing waves should be much longer than the interaction time τ itself, in order to be consistent with the adiabatic approximation on the interactions turn-on and turn-off.

3.6 Atomic lens based on the Berry phase

Next we consider the diffraction of the Gaussian wave packet on the standing waves setup, i.e. first an interaction with the red-detuned wave, and then with the blue-detuned wave. We have shown earlier that in this case the atom in the ground state acquires twice the Berry phase. We now demonstrate that this phase manifests itself in the narrowing of the wave packet. We represent the Gaussian wave packet moving in the y-direction at the initial moment of time by

$$\Psi_0(x) = \frac{1}{\sqrt{\sqrt{\pi}\Delta x_0}} \exp\left(-\frac{x^2}{2\Delta x_0^2}\right) \exp\left[2i\gamma(x)\right], \tag{3.106}$$

where Δx_0 denotes the initial width of the wave-packet and is assumed to be of the order of the laser wave-length $1/k$.

In the momentum representation, the free time evolution of the packet reads

$$\Psi(x,t) = \frac{1}{2\pi\hbar}\int \mathrm{d}p\, C_p \exp\left[\frac{i}{\hbar}\left(px - \frac{p^2}{2M}t\right)\right] \tag{3.107}$$

where

$$C_p = \int \mathrm{d}x'\, \Psi_0(x') \exp\left(-\frac{i}{\hbar}px'\right) \tag{3.108}$$

is determined by the initial condition giving

$$\Psi(x,t) = \frac{1}{2\pi\hbar}\int \mathrm{d}x'\Psi_0(x') \int \mathrm{d}p \exp\left\{\frac{i}{\hbar}\left[p(x-x') - \frac{p^2}{2M}t\right]\right\}. \tag{3.109}$$

According to Eq. (3.82) the geometric phase near the nodes of the standing wave, that is near $x = 0$ in the case of the Eckart envelope is of the form

$$\gamma = \gamma_E = -\pi \ln\left(1 + |\Omega^2|/\Delta^2\right) = -\pi \frac{|\Omega|^2}{\Delta^2} \equiv -\frac{1}{2}\kappa x^2 \tag{3.110}$$

where we have introduced the parameter

$$\kappa \equiv 8\pi k^2 \frac{(\wp \cdot \mathbf{E}_0)^2}{\hbar^2 \Delta^2}. \tag{3.111}$$

When we substitute the expression for the initial wave function, Eq. (3.106), into Eq. (3.109) and use the well-known integral relation

$$\int_{-\infty}^{+\infty} \mathrm{d}p \, \exp(-ap^2 + bp) = \sqrt{\frac{\pi}{a}} \exp(b^2/4a), \tag{3.112}$$

we obtain the time-dependent distribution of finding an atom with the coordinate x

$$|\Psi(x,t)|^2 = \frac{1}{\sqrt{\pi}\Delta x(t)} \exp\left(-\frac{x^2}{2\Delta x^2(t)}\right), \tag{3.113}$$

where the width of the packet $\Delta x(t)$ is determined by the initial width Δx_0 and the Berry phase contribution

$$\Delta x(t) \equiv \Delta x_0 \sqrt{\left(1 - b\frac{t}{t_{spr}}\right)^2 + \left(\frac{t}{t_{spr}}\right)^2} \tag{3.114}$$

where

$$b \equiv 2\kappa \Delta x_0^2 = 16\pi \frac{(\wp \cdot \mathbf{E}_0)^2}{\hbar^2 \Delta^2} (k\Delta x_0)^2 \tag{3.115}$$

results from the Berry phase, Eq. (3.110) and Eq. (3.111), The characteristic time of spreading

$$t_{spr} \equiv M\Delta x_0^2/\hbar \tag{3.116}$$

is determined by the initial width of the packet Δx_0 and the mass of the atom. The minimal possible width of the packet

$$\Delta x_{min} = \frac{\Delta x_0}{\sqrt{1+b^2}} \tag{3.117}$$

is reached at the critical time

$$t_{cr} \equiv \frac{b}{1+b^2} t_{spr}. \tag{3.118}$$

In the Fig. 3.4, we present the Berry phase induced narrowing of the atomic wave-packet for relatively small values of the shrinking parameter b. For example, according

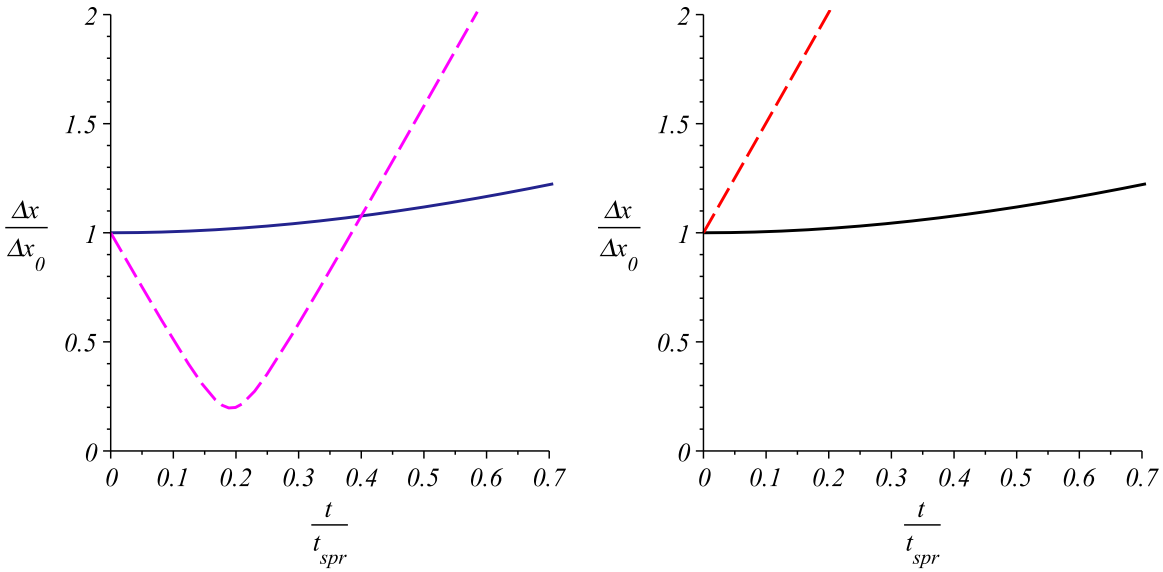


Figure 3.4:
(left): Focusing of the packet (dashed line) due to the geometric phase. Atoms have been prepared in the ground state. $b = 5$.
(right): Fast spreading of the packet for atoms prepared in the excited state (dashed line). $b = 5$.
Solid lines (both left and right) correspond to the propagation of the free Gaussian packet.

to Eq. (3.115) the value $b \approx 5$ is achieved for the Rabi frequency, $\Omega \sim 0.3\Delta$, and the initial packet width, $\Delta x_0 \sim 1/k$. The expression for the minimal packet width, Eq. (3.117) predicts a shrinking up to 5 times compared to the initial width for the parameter $b = 5$. Not surprisingly, the packet expands faster after the critical point than a Berry phase free packet would do. This rapid spreading, however, can be easily understood recalling the Heisenberg uncertainty principle.

We finally turn to the excited state. It is easy to derive a similar formula as for the ground state evolution. However, now the narrowing parameter b appears with the opposite sign. This difference in sign leads to the accelerated spreading of the wave packet, as shown in Fig. 3.4.

Chapter 4

Alternative approaches

4.1 WKB approach in the adiabatic case

Here we present an alternative approach based on the WKB method to derive the results obtained in Sec. 3.4 within Berry's formalism.

We solve the Schrödinger equation,

$$\mathrm{i}\hbar\frac{\mathrm{d}}{\mathrm{d}t}|\Psi(t)\rangle = \left(\hat{H}_a - \mathbf{d}\cdot\mathbf{E}\right)|\Psi(t)\rangle. \tag{4.1}$$

and make the ansatz

$$|\Psi(t)\rangle = A_g^{(WKB)}(t;\mathbf{r})\mathrm{e}^{-\mathrm{i}(\omega_g+\tilde{\Delta}/2)t}|g\rangle + A_e^{(WKB)}(t;\mathbf{r})\mathrm{e}^{-\mathrm{i}(\omega_e-\tilde{\Delta}/2)t}|e\rangle \tag{4.2}$$

which is slightly different from the ansatz Eq. (3.10) Here the effective detuning

$$\tilde{\Delta} \equiv \Delta + \omega_\alpha \tag{4.3}$$

is "shifted" compared to the detuning Δ defined by Eq. (3.8) .

Substituting this ansatz (4.2) into the Schrödinger equation, Eq. (4.1), and following the rotating wave approximation procedure discussed in Sec. 3.1.2, we arrive at

$$\mathrm{i}\hbar\frac{\mathrm{d}}{\mathrm{d}t}\begin{pmatrix}A_e^{(WKB)}\\ A_g^{(WKB)}\end{pmatrix} = \frac{\hbar}{2}\begin{pmatrix}\tilde{\Delta} & V_A\\ V_A & -\tilde{\Delta}\end{pmatrix}\begin{pmatrix}A_e^{(WKB)}\\ A_g^{(WKB)}\end{pmatrix}, \tag{4.4}$$

where the coupling matrix element

$$V_A(t;\mathbf{r}) \equiv \Omega(x)f(t) = \frac{1}{\hbar}V\mathrm{e}^{\mathrm{i}\omega_\alpha t} \tag{4.5}$$

depends on time only through the time dependence $f(t)$ of the envelope, describing the adiabatic turn-on and turn-off of the interaction. In order to transform the system

of two first order differential equations Eq. (4.4) into the second order differential equation for only a single function, we substitute

$$u = \frac{1}{2}(A_g^{(WKB)} + A_e^{(WKB)}) \tag{4.6}$$

and

$$v = \frac{1}{2}(A_e^{(WKB)} - A_g^{(WKB)}), \tag{4.7}$$

into the system Eq. (4.4) and arrive at

$$2\mathrm{i}\dot{u} = \tilde{\Delta}v + V_A u \tag{4.8}$$

and

$$2\mathrm{i}\dot{v} = \tilde{\Delta}u - V_A v. \tag{4.9}$$

Expressing v in terms of u and substituting it into Eq.(4.9) we obtain the second order differential equation

$$\ddot{u} + \frac{1}{4}\left(\tilde{\Delta}^2 + V_A^2 + 2\mathrm{i}\dot{V}_0\right)u = 0 \tag{4.10}$$

for $u(t)$. Next we cast this equation into a form similar to the well-known stationary Schrödinger equation for the coordinate-dependent wave function. For this purpose, we introduce the dimensionless variable $\tilde{t} \equiv t/\tau$, where τ is the duration of the interaction, or the characteristic time for the envelope $f(t)$. Now we rewrite Eq. (4.10) in terms of this dimensionless variable $\tilde{t}$

$$\frac{1}{\tau^2}\frac{\mathrm{d}^2 u}{\mathrm{d}\tilde{t}^2} + \left(\tilde{\varepsilon}^2 + \frac{\mathrm{i}}{2\tau}\frac{\mathrm{d}V_A}{\mathrm{d}\tilde{t}}\right)u = 0, \tag{4.11}$$

where we have introduced the function

$$\tilde{\varepsilon}(\tilde{t}) \equiv \frac{1}{2}\sqrt{\tilde{\Delta}^2 + V_A^2(\tilde{t})}, \tag{4.12}$$

analogous to the quasienergy Eq.(3.27).

The term $\tilde{\varepsilon}^2\tau^2$ is large due to the adiabaticity condition $\Delta\tau \gg 1$. Hence, it is legitimate to use the semiclassical approach. Indeed, one can consider Eq. (4.11) as analogous to the stationary one-dimensional Schrödinger equation where $\tilde{t}$ and $\tilde{\varepsilon}$ play role of the "effective coordinate" and "effective momentum", respectively [81]. The small parameter $1/\tau$ plays here the same role as Planck's constant $\hbar$ in the conventional WKB approach. Therefore, we look for the solution $u(\tilde{t})$ in the semiclassical form $\exp[i\tau S(\tilde{t})]$, resulting in the equation

$$\frac{1}{i\tau}\frac{\mathrm{d}^2 S}{\mathrm{d}\tilde{t}^2} - \left(\frac{\mathrm{d}S}{\mathrm{d}\tilde{t}}\right)^2 + \tilde{\varepsilon}^2 + \frac{\mathrm{i}}{2\tau}\frac{\mathrm{d}V_A}{\mathrm{d}\tilde{t}} = 0 \tag{4.13}$$

for $S(\tilde{t})$. Following the standard procedure, which assumes that the second derivative of S and the last term in Eq. (4.13) small, we present the solution of Eq. (4.13) in the form of the perturbation series in small $1/\tau$:

$$S(\tilde{t}) = S^{(0)}(\tilde{t}) + \frac{1}{\tau} S^{(1)}(\tilde{t}) + \frac{1}{\tau^2} S^{(2)}(\tilde{t}) + ... \tag{4.14}$$

We find the zero-order term

$$S^{(0)}(\tilde{t}) = \pm \int\limits_{-T/\tau}^{\tilde{t}} \mathrm{d}\tilde{t}' \, \tilde{\varepsilon}(\tilde{t}') \tag{4.15}$$

and the first adiabatic correction

$$S^{(1)}(\tilde{t}) = \frac{\mathrm{i}}{2} \ln \left[\tilde{\varepsilon}(\tilde{t}) \left(\frac{V_A(\tilde{t})}{|\tilde{\Delta}|} + \sqrt{1 + \frac{V_A^2(\tilde{t})}{\tilde{\Delta}^2}} \right) \right]. \tag{4.16}$$

The next corrections to the function $S(\tilde{t})$, Eq. (4.14), give negligible contributions to the function $u(\tilde{t})$, i.e. $\exp(\mathrm{i}S^{(2)}/\tau) \simeq 1$, etc. Therefore, the general solution of Eq. (4.11) can be written in the form

$$u(\tilde{t}) = \frac{1}{\sqrt{\mathcal{N}(\tilde{t})\tilde{\varepsilon}(\tilde{t})}} \left\{ A \exp \left[\mathrm{i}\tau \int\limits_{-T/\tau}^{\tilde{t}} \mathrm{d}\tilde{t}' \, \tilde{\varepsilon}(\tilde{t}') \right] + B \exp \left[-\mathrm{i}\tau \int\limits_{-T/\tau}^{\tilde{t}} \mathrm{d}\tilde{t}' \, \tilde{\varepsilon}(\tilde{t}') \right] \right\}, \tag{4.17}$$

where we introduced the normalization function

$$\mathcal{N}(\tilde{t}) \equiv \frac{V_A(\tilde{t})}{|\tilde{\Delta}|} + \sqrt{1 + \frac{V_A^2(\tilde{t})}{\tilde{\Delta}^2}}. \tag{4.18}$$

We can obtain the coefficients A and B recalling the initial conditions $A_g^{(WKB)}(-T) = 1$ and $A_e^{(WKB)}(-T) = 0$, where $T \to +\infty$, and the connection between the function u and the amplitude probabilities $A_g^{(WKB)}$ and $A_e^{(WKB)}$, follows from Eqs. (4.6) and (4.7). Indeed, substituting the initial conditions $A_g^{(WKB)}(-\infty) = 1$ and $A_e^{(WKB)}(-\infty) = 0$ into the system Eqs. (4.6) and (4.7) we determine the initial conditions

$$u(-\infty) = \frac{1}{2}, \tag{4.19}$$

$$v(-\infty) = -\frac{1}{2} \tag{4.20}$$

for the functions u and v. When we substitute these results into Eq. (4.8) we obtain the initial condition

$$\dot{u}(-\infty) = \frac{\mathrm{i}\tilde{\Delta}\tau}{4} \tag{4.21}$$

for the first derivative of the function u. Substituting the expression for u, Eq. (4.17), into Eqs. (4.19)-(4.21) we obtain the coefficients

$$A = \frac{1}{4}\sqrt{\frac{\tilde{\Delta}}{2}}(1+\mathrm{sgn}\tilde{\Delta}) \tag{4.22}$$

and

$$B = \frac{1}{4}\sqrt{\frac{\tilde{\Delta}}{2}}(1-\mathrm{sgn}\tilde{\Delta}), \tag{4.23}$$

which lead us to the explicit form

$$\begin{aligned} u(\tilde{t}) &= \frac{1}{\sqrt{\mathcal{N}(\tilde{t})\tilde{\varepsilon}(\tilde{t})}}\frac{1}{4}\sqrt{\frac{\tilde{\Delta}}{2}}\left\{(1+\mathrm{sgn}\tilde{\Delta})\exp\left[\mathrm{i}\tau\int\limits_{-T/\tau}^{\tilde{t}}\mathrm{d}\tilde{t}'\,\tilde{\varepsilon}(\tilde{t}')\right]+\right. \\ &\left.+(1-\mathrm{sgn}\tilde{\Delta})\exp\left[-\mathrm{i}\tau\int\limits_{-T/\tau}^{\tilde{t}}\mathrm{d}\tilde{t}'\,\tilde{\varepsilon}(\tilde{t}')\right]\right\} \end{aligned} \tag{4.24}$$

of the solution. The same procedure can be made with respect to the function v, giving

$$\begin{aligned} v(\tilde{t}) &= -\frac{1}{\sqrt{\mathcal{N}(\tilde{t})\tilde{\varepsilon}(\tilde{t})}}\frac{1}{4}\sqrt{\frac{\tilde{\Delta}}{2}}\left\{(1+\mathrm{sgn}\tilde{\Delta})\exp\left[\mathrm{i}\tau\int\limits_{-T/\tau}^{\tilde{t}}\mathrm{d}\tilde{t}'\,\tilde{\varepsilon}(\tilde{t}')\right]+\right. \\ &\left.+(1-\mathrm{sgn}\tilde{\Delta})\exp\left[-\mathrm{i}\tau\int\limits_{-T/\tau}^{\tilde{t}}\mathrm{d}\tilde{t}'\,\tilde{\varepsilon}(\tilde{t}')\right]\right\}. \end{aligned} \tag{4.25}$$

From Eqs. (4.24) and (4.25) we deduce the symmetry relation $v(\tilde{t}) = -u(\tilde{t})$, which confirms that there are no transitions into the excited state. Indeed, substituting the expressions for the functions u and v into the system Eqs. (4.6) and (4.7), we obtain

$$A_e^{(WKB)}(\tilde{t}) = u(\tilde{t}) + v(\tilde{t}) = 0 \tag{4.26}$$

and

$$A_g^{(WKB)}(\tilde{t}) = u(\tilde{t}) - v(\tilde{t}) = 2u(\tilde{t}). \tag{4.27}$$

When we return to the time variable t, we obtain

$$\begin{aligned} A_g^{(WKB)}(t) &= \frac{1}{\sqrt{\mathcal{N}(t)\tilde{\varepsilon}(t)}}\frac{1}{4}\sqrt{\frac{\tilde{\Delta}}{2}}\left\{(1+\mathrm{sgn}\tilde{\Delta})\exp\left[\mathrm{i}\int\limits_{-T}^{t}\mathrm{d}t'\,\tilde{\varepsilon}(t')\right]+\right. \\ &\left.+(1-\mathrm{sgn}\tilde{\Delta})\exp\left[-\mathrm{i}\tau\int\limits_{-T}^{\tilde{t}}\mathrm{d}\tilde{t}'\,\tilde{\varepsilon}(\tilde{t}')\right]\right\}. \end{aligned} \tag{4.28}$$

We recall from Eq. (4.2) the prefactors $\exp[-\mathrm{i}(\omega_g \pm \tilde{\Delta}/2)t]$ and obtain that during the time $2T$ the ground state exponential prefactor gives a contribution to the ground state phase equal to $-\tilde{\Delta}T$. As in chapter 3 we neglect the contribution of the $-\mathrm{i}\omega_g t$ term as it is irrelevant in an interference experiment. Summing it up with the part acquired due to the atom-field interaction Eq. (4.28) the total phase acquired by the ground state reads

$$\varphi_g^{(WKB)}(T \to \infty) \equiv \lim_{T\to\infty} \left[\exp(-\mathrm{i}\tilde{\Delta}T) A_g^{(WKB)}(T)\right]. \tag{4.29}$$

Next we make a Taylor expansion of this expression for small ω_α^2, as for example in the expression for the quasienergy

$$\begin{aligned}
\sqrt{\tilde{\Delta}^2 + V_A^2} &= \sqrt{\Delta^2 + V_A^2}\sqrt{1 + \frac{2\Delta\omega_\alpha}{\Delta^2 + V_A^2}} \\
&= \sqrt{\Delta^2 + V_A^2}\left(1 + \frac{\Delta\omega_\alpha}{\Delta^2 + V_A^2}\right) \\
&= |\Delta|\sqrt{1 + a^2 f^2(t)} + \omega_\alpha \mathrm{sgn}\Delta \frac{1}{\sqrt{1 + a^2 f^2(t)}}.
\end{aligned} \tag{4.30}$$

Afterwords, we obtain the WKB-probability amplitude

$$\varphi_g^{(WKB)}(\infty) = \exp\left[i\frac{\Delta}{2}\int_{-\infty}^{+\infty} \mathrm{d}t\ \left(\sqrt{1 + a^2 f^2(t)} - 1\right) + i\frac{\omega_\alpha}{2}\int_{-\infty}^{+\infty} \mathrm{d}t\ \left(\frac{1}{\sqrt{1 + a^2 f^2(t)}} - 1\right)\right] \tag{4.31}$$

of finding the atom in the ground state after the scattering by the standing wave. This expression coincides with the one discussed in Sec. 3.4 and based on Berry's approach. We recognize that the phase factor in the first exponential on the right-hand side of the expression for the probability amplitude of the ground state, Eq. (4.31), coincides with the expression Eq. (3.101) for the dynamical phase of the Berry's approach and the phase factor of the second exponential coinsides with the geometric phase given by Eq. (3.102).

4.2 Berry's approach and atomic state method: A comparison

One might introduce an even more elementary way of solving the Schrödinger equation in the case of a vanishing decay rate from the excited level. Indeed, we now consider the regime of a weak interaction field and hence weak saturation of the excited level.

Next we would like to check if the result obtained within this approach will coincide with the results demonstrated above within the WKB method and Berry's approach.

Substituting an ansatz

$$|\Psi(t)\rangle \equiv A_g^{(A)}(t;\mathbf{r})\mathrm{e}^{-\mathrm{i}\omega_g t}|g\rangle + A_e^{(A)}(t;\mathbf{r})\mathrm{e}^{-\mathrm{i}(\omega_e-\tilde{\Delta})t}|e\rangle \tag{4.32}$$

into the Schrödinger equation (3.9) and using the rotating wave approximation, we obtain

$$\mathrm{i}\frac{\partial A_e^{(A)}}{\partial t} = \tilde{\Delta}A_e^{(A)} + \frac{V_A}{2}A_g^{(A)} \tag{4.33}$$

and

$$\mathrm{i}\frac{\partial A_g^{(A)}}{\partial t} = \frac{V_A}{2}A_e^{(A)}. \tag{4.34}$$

Here, we use the designations for $\tilde{\Delta}$ and V_A introduced by Eqs. (4.3) and (4.5), respectively.

Next we neglect the derivative $\partial A_e^{(A)}/\partial t$ in Eq. (4.33). Since due to the weakness of the interaction field we have the inequality $V_0/\tilde{\Delta} \ll 1$. Substituting $A_e^{(A)}$, which is expressed in terms of $A_g^{(A)}$ from Eq. (4.33) into Eq. (4.34) we obtain the system

$$A_e^{(A)} = -\frac{V_A}{2\tilde{\Delta}}A_g^{(A)} \tag{4.35}$$

and

$$\mathrm{i}\frac{\partial A_g^{(A)}}{\partial t} = -\frac{V_A^2}{4\tilde{\Delta}}A_g^{(A)} \tag{4.36}$$

of equations. It is straightforward to solve Eq. (4.36) giving

$$A_g^{(A)}(+T) = A_g^{(A)}(-T)\exp\left[\mathrm{i}\frac{a^2}{4}(\Delta-\omega_\alpha)\int_{-T}^{+T}\mathrm{d}t f^2(t)\right] \tag{4.37}$$

Here we recognize the sum of the dynamical phase given by the first term in the exponential and the geometric phase represented by the second term in the exponential in complete agreement with the expressions presented in Sec. 3.4.3 in the weak field limit ($a \ll 1$). However, if we return now to the excited state probability, we will find out taking into account the relation Eq.(4.35) that the probability amplitude for finding atom in the excited state reads

$$A_e^{(A)}(+T) = A_e^{(A)}(-T)\frac{f(+T)}{f(-T)}\exp\left[\mathrm{i}\frac{a^2}{4}(\Delta-\omega_\alpha)\int_{-T}^{+T}\mathrm{d}t f^2(t)\right]. \tag{4.38}$$

Indeed, this result differs from those obtained within the WKB method and Berry's approach. Hence, the atomic state approach allows us to obtain only the phase factor of the ground state correctly. To neglect of the first derivative of the excited state

probability amplitude in the system of Eqs. (4.33) and (4.34) is responsible for this flaw.

In the Table 4.1, we summarize the results obtained within the Berry dressed states and the atomic states approaches. In the dressed state approach one obtains the dynamical and geometric contributions independently from each other. On a contrary, the phase obtained within the atomic state approach is obtained as a whole expression. However, it is possible to distinguish between the time-dependent (proportional to Δ term) and time-independent (proportional to ω_α term) contributions, corresponding to the dynamical and geometric phases of dressed state approach, obtained in the weak limit, respectively. Although this correspondence holds for the ground state phase, the excited state phase could not be obtained correctly in the atomic states approach. This fact emphasizes the usefulness and generality of the Berry's dressed states approach.

Phase	Dressed state approach		Atomic state approach
	exact	weak	
Dynamical			
ground	β	β_w	___
excited	$-\beta$	$-\beta_w$	
Geometrical			
ground	γ	γ_w	___
excited	$-\gamma$	$-\gamma_w$	
Total			
ground	$\gamma+\beta$	$\gamma_w+\beta_w$	$\gamma_w+\beta_w$
excited	$-(\gamma+\beta)$	$-(\gamma_w+\beta_w)$	$\gamma_w+\beta_w$

Table 4.1: Comparison between the phases calculated within the dressed state and atomic state approaches. Dynamical phase β acquired by the ground level in the exact dressed state approach calculation reduces to the β_w in the approximation of the weak field. The total phase for the ground state, which is a sum of the dynamical β_w and geometric parts γ_w in the weak limit, coincide with the one obtained in the atomic state approach, where the excitation was neglected from the beginning. This coincidence, however does not take place for the excited state.

Chapter 5

Scattering from a traveling wave

In the following chapter we would like to expand our analysis by considering the scattering of a two-level atom from a traveling wave and by taking into account the kinetic energy operator. First we obtain an exact solution in the case of the inverse-cosh envelope of the field. Then we demonstrate that the same results could be received within Berry's approach. In conclusion, we compare these results with running waves to those obtained for standing waves.

5.1 Schrödinger equation

We consider the scattering of a two-level atom by a near-resonant running light wave.

The running wave is situated along the x-axis and the average velocity of the atomic wave packet is directed at some small angle α measured relative to the y-axis, that is $\mathbf{v} = \{v\sin\alpha, v\cos\alpha, 0\}$.

The electric field of the wave with frequency ω reads

$$\mathbf{E}(\mathbf{r},t) = \mathbf{E}_0\cos(kx-\omega t) \tag{5.1}$$

and the polarization vector $\mathbf{E}_0$ is aligned along the z-axis.

The time evolution of the state vector $|\Psi\rangle$ of the two-level atom interacting with the electromagnetic field follows Eq. (3.2).

The atom propagates with the macroscopic velocity $\mathbf{v} = \{v\sin\alpha, v\cos\alpha\}$, where the angle α is relatively small. For this reason we treat this motion classically along the y-axis that is $y = v_y t$. In contrast the motion along the x-axis is described quantum mechanically. Substituting the ansatz

$$|\Psi(\mathbf{r},t)\rangle = A_g^{(r)}(t;\mathbf{r})\mathrm{e}^{-\mathrm{i}\omega_g t}|g\rangle + A_e^{(r)}(t;\mathbf{r})\mathrm{e}^{-\mathrm{i}\omega_e t}|e\rangle \tag{5.2}$$

into the Schrödinger equation (3.2) we arrive at the system of equations

$$\mathrm{i}\hbar\frac{\partial A_e^{(r)}}{\partial t} = \hat{H}_{cm}A_e^{(r)} - \wp\cdot\mathbf{E}\,A_g^{(r)}\mathrm{e}^{i(\omega_e-\omega_g)t} \tag{5.3}$$

and

$$\mathrm{i}\hbar\frac{\partial A_g^{(r)}}{\partial t} = \hat{H}_{cm}A_g^{(r)} - \wp\cdot\mathbf{E}\,A_e^{(r)}\mathrm{e}^{-i(\omega_e-\omega_g)t} \tag{5.4}$$

determining the spatial- and time-dependent coefficients $A_g^{(r)}(x,y,t)$ and $A_e^{(r)}(x,y,t)$ where we have introduced the dipole matrix element $\wp \equiv \langle g|\mathbf{d}|e\rangle$. Next we substitute the exact time dependence of the electromagnetic field given by Eq. (5.1) and make the rotating wave approximation, that is we neglect the terms depending on $\exp\{\pm 2\mathrm{i}\omega t\}$, which results in

$$\mathrm{i}\hbar\frac{\partial A_e^{(r)}}{\partial t} = \hat{H}_{cm}A_e^{(r)} - \frac{\wp\cdot\mathbf{E}_0}{2}\,A_g^{(r)}\mathrm{e}^{i(\Delta t+kx)} \tag{5.5}$$

and

$$\mathrm{i}\hbar\frac{\partial A_g^{(r)}}{\partial t} = \hat{H}_{cm}A_g^{(r)} - \frac{\wp\cdot\mathbf{E}_0}{2}\,A_e^{(r)}\mathrm{e}^{-i(\Delta t+kx)}. \tag{5.6}$$

After introducing the ansatz

$$A_e^{(r)}(x,y,t) = \tilde{A}_e^{(r)}(y)\exp\left\{\frac{\mathrm{i}}{\hbar}\left[-\frac{\mathbf{p}^2}{2M}t + (\mathbf{p}+\hbar\mathbf{k})\cdot\mathbf{r} + \frac{\Delta}{2}t\right]\right\} \tag{5.7}$$

and

$$A_g^{(r)}(x,y,t) = \tilde{A}_g^{(r)}(y)\exp\left[\frac{\mathrm{i}}{\hbar}\left(-\frac{\mathbf{p}^2}{2M}t + \mathbf{p}\cdot\mathbf{r} - \frac{\Delta}{2}t\right)\right], \tag{5.8}$$

we arrive at

$$\mathrm{i}\hbar v_y\frac{\partial \tilde{A}_e^{(r)}}{\partial y} = \hbar\left(\frac{\Delta}{2} + \frac{\hbar k^2}{2M} + \frac{kp_x}{M}\right)\tilde{A}_e^{(r)} - \frac{\wp\cdot\mathbf{E}_0}{2}\,\tilde{A}_g^{(r)} \tag{5.9}$$

and

$$\mathrm{i}\hbar v_y\frac{\partial \tilde{A}_g^{(r)}}{\partial y} = -\hbar\frac{\Delta}{2}\tilde{A}_g^{(r)} - \frac{\wp\cdot\mathbf{E}_0}{2}\,\tilde{A}_e^{(r)}. \tag{5.10}$$

Here the second derivatives $\partial^2\tilde{A}_{e,g}^{(r)}/\partial y^2$ are neglected, which is allowed due to the smoothness of the functions $\tilde{A}_{e,g}^{(r)}$. Moreover, as in Chapter 3, we deal now with the effective time $t \equiv y/v_y$. Hence, we can write $\mathbf{E_0}(y) \equiv \mathbf{E_0}(vt)$ and Eqs. (5.9) and (5.10) take the form

$$\mathrm{i}\hbar\frac{\mathrm{d}\tilde{A}_e^{(r)}}{\mathrm{d}t} = \hbar\left(\frac{\Delta}{2} + \omega_{rec} + \omega_\alpha\right)\tilde{A}_e^{(r)} - \frac{\wp\cdot\mathbf{E}_0}{2}\,\tilde{A}_g^{(r)} \tag{5.11}$$

and

$$\mathrm{i}\hbar\frac{\mathrm{d}\tilde{A}_g^{(r)}}{\mathrm{d}t} = -\hbar\frac{\Delta}{2}\tilde{A}_g^{(r)} - \frac{\wp\cdot\mathbf{E}_0}{2}\,\tilde{A}_e^{(r)}, \tag{5.12}$$

where we have recalled the expressions Eq. (3.6) and Eq. (3.19 for the recoil frequency ω_{rec} and the Doppler frequency ω_α), respectively. The boundary conditions are given by the fact that the interaction is absent when $y \to -\infty$, that is $t \to -\infty$, giving $\tilde{A}_g^{(r)} = 1$ and $\tilde{A}_e^{(r)} = 0$.

5.2 Transition to Berry's formalism

In this section we return to Berry's description and find solutions of the Schrödinger equation, that is, obtain the phases aquired by the atom during the interaction with the running wave.

For this purpose we make the transformation

$$\tilde{A}_e^{(r)} = \tilde{A}_e^{(r,B)} \mathrm{e}^{-i\tilde{\omega}_\alpha t} \tag{5.13}$$

and

$$\tilde{A}_g^{(r)} = \tilde{A}_g^{(r,B)} \tag{5.14}$$

leading to the Berry's type of Hamiltonian where we have introduced $\tilde{\omega}_\alpha \equiv \omega_\alpha + \omega_{rec}$, which leads to

$$\mathrm{i}\hbar \frac{\mathrm{d}\tilde{A}_e^{(r,B)}}{\mathrm{d}t} = \hbar \frac{\Delta}{2} \tilde{A}_e^{(r,B)} - \frac{\wp \cdot \mathbf{E}_0}{2} \mathrm{e}^{i\tilde{\omega}_\alpha t}\, \tilde{A}_g^{(r,B)} \tag{5.15}$$

and

$$\mathrm{i}\hbar \frac{\mathrm{d}\tilde{A}_g^{(r,B)}}{\mathrm{d}t} = -\hbar \frac{\Delta}{2} \tilde{A}_g^{(r,B)} - \frac{\wp \cdot \mathbf{E}_0}{2} \mathrm{e}^{-i\tilde{\omega}_\alpha t}\, \tilde{A}_e^{(r,B)}. \tag{5.16}$$

Introducing an interaction-describing term

$$V_r = V_r(t) \equiv \wp \cdot \mathbf{E}_0(t) \mathrm{e}^{-i\tilde{\omega}_\alpha t} \tag{5.17}$$

we arrive at

$$\mathrm{i}\hbar \frac{\mathrm{d}}{\mathrm{d}t} \begin{pmatrix} \tilde{A}_e^{(r,B)} \\ \tilde{A}_g^{(r,B)} \end{pmatrix} = \hat{H}_r \begin{pmatrix} \tilde{A}_e^{(r,B)} \\ \tilde{A}_g^{(r,B)} \end{pmatrix}, \tag{5.18}$$

with the Berry-like Hamiltonian

$$\hat{H}_r = \frac{1}{2} \begin{pmatrix} \hbar\Delta & V_r^* \\ V_r & -\hbar\Delta \end{pmatrix}. \tag{5.19}$$

These equations are similar to Eqs. (3.11) and (3.12). Now we can recall the results obtained in Chapter 3 and use the analogy between Eqs. (3.11) and (5.18). Indeed, the formulae for the acquired dynamical and geometric phases in the case of a running wave differ from those of the standing wave case by $\tilde{\omega}_\alpha$ instead of ω_α and V_r instead of V.

5.2.1 Geometric and dynamical phases

The interaction term

$$V_r(t;\mathbf{r}) = \hbar\Omega_0 f(t)\mathrm{e}^{-\mathrm{i}\tilde{\omega}_\alpha t} \tag{5.20}$$

differs from that of equation Eq. (3.24) by

$$\frac{V}{V_r} = \frac{\Omega}{\Omega_0}\mathrm{e}^{\mathrm{i}\omega_{rec}t}, \tag{5.21}$$

where, recalling expressions for the Rabi frequencies Ω and Ω_0, Eqs. (3.23) and (2.12), respectively, we find

$$\frac{\Omega}{\Omega_0} = 2\sin(kx\cos\alpha). \tag{5.22}$$

That is we arrive at the expressions for the geometric and dynamical phases, compare with Eq. (3.58) and Eq. (3.86),

$$\gamma^{(r)} = \frac{1}{2}\int\limits_{\phi_i}^{\phi_f} \mathrm{d}\phi \left[\frac{1}{\sqrt{1+a_0^2(x)f^2(\phi/\tilde{\omega}_\alpha)}} - 1\right] \tag{5.23}$$

and

$$\beta^{(r)} = |\Delta| \int\limits_0^{+T} \mathrm{d}t \left(\sqrt{1+a_0^2 f^2(t)} - 1\right), \tag{5.24}$$

respectively. Here we have introduced the new dimensionless

$$a_0 \equiv \frac{|\Omega_0|}{|\Delta|} \tag{5.25}$$

Rabi frequency, which is independent of the x-coordinate, in contrast to $a(x)$ in Chapter 3.

We notice that a new condition for having the closed circuit $\tilde{\omega}_\alpha\tau_r = 2\pi$ in the parameter space is necessary here, compare with the condition Sec. 3.3 where the circuit is only closed provided $\omega_\alpha\tau = 2\pi$. Therefore, the characteristic time of interaction τ_r in the case of two-level atom scattering by a running wave should differ from that of the standing wave case by

$$\frac{\tau}{\tau_r} = \frac{\tilde{\omega}_\alpha}{\omega_\alpha} = 1 + \frac{\omega_{rec}}{\omega_\alpha} = 1 + \frac{\hbar k}{2Mv\sin\alpha} \tag{5.26}$$

in order to compare the phases acquired in both cases. Here it is worthwhile to remind that the angle α is small, $\alpha \ll 1$

With the connection settled between the geometric and dynamical phases acquired in the atom scattering by standing wave, Eq. (3.58) and Eq. (3.86), and those phases acquired in the atom scattering by running wave, Eq. (5.23) and Eq. (5.24), respectively, we are able to present the corresponding results for the different envelopes of the running wave field.

Mesa envelope

The mesa envelope f_M given by Eq. (3.48) is non-vanishing and constant only for the time interval $-\tau_r/2 < t < \tau_r/2$. Recalling Eq. (3.62) and Eq. (3.88) we obtain the expressions

$$\gamma_M^{(r)} = \pi \left(\frac{1}{\sqrt{1+a_0^2}} - 1 \right) \tag{5.27}$$

for the geometric phase and

$$\beta_M^{(r)} = \frac{\pi|\Delta|}{\tilde{\omega}_\alpha} \left(\sqrt{1+a_0^2} - 1 \right) \tag{5.28}$$

for the dynamical phase. In the weak-field limit $a_0^2 \ll 1$ we arrive at

$$\gamma_M^{(r)} = \sigma_M a_0^2 \pi \tag{5.29}$$

and

$$\beta_M^{(r)} = \frac{\pi|\Delta|}{2\tilde{\omega}_\alpha} a_0^2, \tag{5.30}$$

where we have used the abbreviation $\sigma_M \equiv -1/2$ as in the chapter 3.

Squared-cos potential

We now turn to the envelope of the form of the squared-cosine potential given by Eq. (3.49). In the case of the squared-cosine potential envelope given by Eq. (3.49) the circuit in parameter space is a cardioid and the integral Eq. (5.23) determining the geometric phase takes the form

$$\gamma_C^{(r)} = \frac{2}{(a_0^2+1)^{1/4}} \mathrm{K}\left(\frac{1}{\sqrt{2}} \sqrt{1 - \frac{1}{\sqrt{a_0^2+1}}} \right) - \pi. \tag{5.31}$$

For $a_0 \ll 1$ gives

$$\gamma_C^{(r)} = \sigma_C a_0^2 \pi, \tag{5.32}$$

where we use the abbreviation $\sigma_C \equiv -3/16$, which was introduced in the chapter 3. For the sake of simplicity, we show the result for the dynamical phase already in the weak-field limit $a_0^2 \ll 1$

$$\beta_C^{(r)} = \frac{3\pi|\Delta|}{16\tilde{\omega}_\alpha} a_0^2. \tag{5.33}$$

Eckart envelope

In the case of the Eckart envelope the expression for the geometric phase Eq. (5.23) takes the form

$$\gamma_E^{(r)} = -\pi \ln(1 + a_0^2). \tag{5.34}$$

In the weak-field limit $a_0 \ll 1$ and for $\tilde{\omega}_\alpha \tau_r$, we obtain

$$\gamma_E^{(r)} = \sigma_E a_0^2 \pi \tag{5.35}$$

with the numerical factor $\sigma_E \equiv -1$.

The dynamical phase is given by the expression

$$\beta_E^{(r)} = \frac{2\pi|\Delta|}{\tilde{\omega}_\alpha} \left(a_0 \arctan a_0 - \ln \sqrt{1 + a_0^2} \right). \tag{5.36}$$

and should be compared with and contraster to Eq. (3.98) for the case of the standing wave. For $a_0^2 \ll 1$ Eq. (5.36) reduces to

$$\beta_E^{(r)} = \frac{\pi|\Delta|}{\tilde{\omega}_\alpha} a_0^2. \tag{5.37}$$

One notices, that we see the difference between the atomic scattering by the standing (chapter 3) and running waves (current chapter) in the shift of the "effective" Doppler frequency by the recoil frequency $\omega_\alpha \to \tilde{\omega}_\alpha = \omega_\alpha + \omega_{rec}$ and independence of the normalized Rabi frequency a_0 (compare with $a(x)$ of chapter 3) on the atomic center-of-mass position.

5.2.2 Ratio $\gamma^{(r)}/\beta^{(r)}$ in possible experiment

Now we can recall the expression Eq. (3.103) for the ratio between the geometric and dynamical phase in the limit of the weak field $|\Omega| \ll |\Delta|$ and rewrite it for the case of running wave $|\Omega_0| \ll |\Delta|$

$$\left| \frac{\gamma^{(r)}}{\beta^{(r)}} \right| = \left| \frac{\tilde{\omega}_\alpha}{\Delta} \right| = \left| \frac{\gamma}{\beta} \right| + \frac{\omega_{rec}}{\Delta} \simeq 0.101. \tag{5.38}$$

This ratio is even slightly improved comparing to the standing wave case (by 1%). We used here the data for the argon atoms as presented in Sec. 3.4.3.

5.2.3 Cancellation of the dynamical phase

Now we are in the position to propose a scheme for the dynamical phase cancellation in the atomic scattering by running wave. The structure of the expressions for the total

phases acquired by the ground and excited states in the case of scattering by running wave could be shown similar to those of the scattering by standing wave, recall Eq. (3.39) and Eq. (3.41), respectively. Therefore, we suggest the analogous scheme of the dynamical phase cancellation to those which have been shown in chapter 3. Indeed, since the dynamical part depends on the sign of the detuning, we propose to use two consecutive interactions of the atom with the running waves, that is, firstly with the blue detuned wave ($\Delta > 0$), secondly with the red detuned wave ($\Delta' = -\Delta < 0$). Hence, due to the opposite signs of the detuning, the dynamical contributions cancel each other. The geometric phase is summed up after the second scattering. Moreover, on a contrary to the case of the standing wave scattering, we do not need the fulfillment of the additional condition $k\cos\alpha = k'\cos\alpha'$ for the dynamical phase cancellation. This easing is due to the independence of the interaction term V_r Eq. (5.20) on the atomic center-of-mass motion on a contrary to the interaction term of the standing wave case Eq. (3.16).

Thus, in the configuration proposed above for two consecutive scatterings of an atom by the opposite detuned running waves we receive cancellation of the dynamical phase and approximate doubling of the Berry phase. Here, as for the standing waves case, the time interval between two interactions of an atom with standing waves should be much longer than the interaction time τ_r itself, in order to be consistent with the adiabatic approximation on the interactions turn-on and turn-off.

5.3 Exact solution: $1/\cosh$ envelope

Now we are in position to consider the case of the inverse-cosh envelope, for which the exact solution can be obtained, see Chapter 2. Let us first transform the system of equations (5.15) and (5.16) to the form used in Chapter 2, system of equations (2.9) and (2.10) and then apply the solution obtained there for our case. In order to do it, we substitute

$$\tilde{A}_e^{(r,B)} = \tilde{A}_e^{(r,E)} \exp(-\mathrm{i}\Delta t/2), \tag{5.39}$$

$$\tilde{A}_g^{(r,B)} = \tilde{A}_g^{(r,E)} \exp(\mathrm{i}\Delta t/2) \tag{5.40}$$

into the system of equations (5.15) and (5.16) and obtain

$$\mathrm{i}\hbar\frac{\mathrm{d}\tilde{A}_e^{(r,E)}}{\mathrm{d}t} = -\frac{\wp\cdot\mathbf{E}_0}{2}\mathrm{e}^{i(\Delta+\tilde{\omega}_\alpha)t}\,\tilde{A}_g^{(r,E)}, \tag{5.41}$$

$$\mathrm{i}\hbar\frac{\mathrm{d}\tilde{A}_g^{(r,E)}}{\mathrm{d}t} = -\frac{\wp\cdot\mathbf{E}_0}{2}\mathrm{e}^{-i(\Delta+\tilde{\omega}_\alpha)t}\,\tilde{A}_e^{(r,E)}, \tag{5.42}$$

which is indeed of the form Eqs. (2.9) and (2.10). Using the solution Eq. (2.31), we arrive at the equation for the probability amplitude to find an atom in the ground state

$$A_g^{(r,E)} = \exp\left(-\mathrm{i}(\Delta+\tilde{\omega}_\alpha)\tau_r \ln\sqrt{1+\frac{|\Omega_0|^2}{(\Delta+\tilde{\omega}_\alpha)^2}} + \mathrm{i}|\Omega_0|\tau_r \arctan\frac{|\Omega_0|}{(\Delta+\tilde{\omega}_\alpha)}\right). \quad (5.43)$$

with Ω_0 the same as introduced in chapter 2, as shown by Eq. (2.12)

$$\Omega \equiv \frac{\wp\cdot\mathcal{E}_0}{\hbar}, \quad (5.44)$$

where we assumed $\mathbf{E}_0 = \mathcal{E}_0/\cosh(t/\tau_r)$.

Let us now recall the condition $\tilde{\omega}_\alpha\tau_r = 2\pi$ and make a Taylor expansion in $\tilde{\omega}_\alpha/\Delta \ll 1$ in the expression for the phase obtained within the exact solution method Eq. 5.43. That is, we obtain

$$\ln\sqrt{1+\frac{|\Omega_0|^2}{(\Delta+\tilde{\omega}_\alpha)^2}} \simeq \ln\sqrt{1+a_0^2\left(1-\frac{2\tilde{\omega}_\alpha}{\Delta}\right)} \quad (5.45)$$

and

$$\arctan\frac{|\Omega_0|}{(\Delta+\tilde{\omega}_\alpha)} \simeq \arctan\left[a_0\left(1-\frac{\tilde{\omega}_\alpha}{\Delta}\right)\right]. \quad (5.46)$$

Using further the expansion of the ln and arctan- functions

$$\ln(x+h) \simeq \ln x + h\frac{1}{x} \quad (5.47)$$

and

$$\arctan(x+h) \simeq= \arctan x + h\frac{1}{1+x^2} \quad (5.48)$$

we obtain from 5.43

$$A_g^{(r,E)} = \mathrm{e}^{\mathrm{i}(\beta_E^{(r)}\mathrm{sgn}\Delta+\gamma_E^{(r)})}. \quad (5.49)$$

Hence, we have shown that the exact solution in the case of the inverse-cosh envelope coincides with the solution obtained within the Berry's geometric phase approach for the running wave. In the exact solution, one can easily distinguish between the time-dependent part, proportional to the $\tilde{\omega}_\alpha^{-1}$, and time-independent part, which indeed correspond to the dynamical and geometric parts of the Berry's approach, respectively. Therefore, we verified the correctness of applying the Berry's formalism for the atomic scattering by the laser field. Moreover, the Berry's method is valid for any envelope form, which justify it as a much more powerful tool for solving the scattering problems than the exact solution method, which is applicable only for the case of the inverse-cosh envelope function.

5.4 Comparison of the standing and running wave proposals

Let us now summarize the features of the both standing wave and running wave scattering proposals and underline advantages and disadvantages of each approach.

We show in Ch. 3 that the geometric phase acquired in the case of the standing wave scattering is atomic-position dependent, $\gamma = \gamma(x)$, since γ is determined by $|\Omega^2(x)| \propto \sin^2(kx)$, as shown by Eq. (3.58). Therefore, we use this fact to propose an atomic lens construction for the novel non-interferometric observation possibility of this phase. However, due to the complexity of the system our results were obtained and are valid only within the Raman-Nath regime, that is by the neglection of the kinetic energy operator. On the contrary, we take the kinetic energy operator into account in the case of two-level atom scattering by the running wave in the present chapter. Here, we can not have the dependence of the geometric phase on the atomic coordinate though, as it is clear from Eq. (5.23). Therefore, we would not have the atomic lens effect in this case. Hence, only usual interferometric scheme for observation of the geometric phase can be applied.

Both cases allow the opposite detuning based scheme for the dynamical phase cancellation, but the improvement of the geometric phase to dynamical phase ratio in the case of scattering by running wave is negligibly small, as shown by Eq. (5.38).

Moreover, one can show the results obtained for the case of two-level atom scattering by the running wave are deeply connected to the results obtained for the case of two-level atom scattering by the standing wave. As $\tilde{\omega}_\alpha \equiv \omega_\alpha + \omega_{rec}$, then in the case of the infinitely heavy atom, that is $M \to \infty$, we have $\omega_{rec} \to 0$ and $\tilde{\omega}_\alpha \to \omega_\alpha$, which would also correspond to not taking the kinetic energy operator into account, as we did in the case of standing wave. Thinking about an infinitely heavy atom we came to nearly the same formulae, except for the independence of the geometric phase on the atomic coordinate x in the case of running wave, because γ would be determined again by $|\Omega(x)|^2 = |\Omega_0|^2$.

Two proposals seem to be very similar in the outcome, however, the difference between them reveals in the independence on the atomic coordinate x in the case of running wave on a contrary to the standing wave case, where coordinate x is a parameter. This difference occurs due to the different regimes, that is we are within the Raman-Nath regime in the case of standing wave and out of it, while considering the running wave case. As it is shown by Eq. (3.5), the Raman-Nath regime itakes place when the time of interaction τ is small, that is $\tau \ll /\sqrt{\omega_{rec}\Omega_0}$. In this case, we are allowed to neglect the kinetic energy operator. However, for large interaction time $\sqrt{\omega_{rec}\Omega_0} \ll \tau \ll 1/\Gamma$ the kinetic energy operator should be taken into account. Hence, the main factor, determining the difference between the scattering on the running and

standing waves, is the value of the interaction time. It is not a simple task to take a kinetic energy operator into account in the case of standing wave. However, we have shown that the formulae of the running wave case transforms into the formula analogous to those of the standing wave case, but independent on the external atomic degrees of freedom. Therefore, we might deduce, that taking the kinetic energy operator into account in the case of the atomic scattering on the standing wave will not change the values of the dynamical and geometric phases significantly from those we obtained within the Raman-Nath regime.

We would like to emphasize again that in the case of taking the kinetic energy operator into account, that is at long interaction time $\sqrt{\omega_{rec}\Omega_0} \ll \tau \ll 1/\Gamma$, the only possible scheme to detect a Berry phase is to make an interference experiment. The Raman-Nath regime, that is the case of small interaction times $\tau \ll /\sqrt{\omega_{rec}\Omega_0}$, however, enables the atomic lens proposal, which is possible due to the dependence of the geometric phase on the atomic center-of-mass position.

Conclusion

In the present thesis we have considered the scattering of the two-level atom from an appropriately designed electromagnetic field and propose the scheme for the observation of the geometric phase acquired by the two-level atom during the interaction with the scattering field. At first we have reviewed the basic elements of the Berry phase and atom-light interaction. Then we have revealed the occurrence of the geometric phase in our problem. We consider the Berry phase in the scattering of a two-level atom by the near-resonant standing light wave within (i) the rotating wave approximation, (ii) the adiabatic approximation on the atomic center-of-mass motion, and (iii) adiabatically slow switch-on and -off of the interaction. These approximations are valid and self-consistent under the fulfillment of the conditions $\sqrt{1+(\omega_\alpha\tau)^2} \ll \Delta\tau \ll \sqrt{\Delta/\omega_{rec}}$ and $\Gamma\tau w \leq 1$, which we discussed in Sec. 3.1.1.

In Sec. 3.4.3 we have provided estimates for typical experimental values of the system which make the ratio of the Berry phase to dynamical phase to be approximately 0.1, which make it feasible to observe the Berry phase in suggested experiment. Moreover, we propose a novel scheme of the dynamical phase cancellation, achieved by the employment of the oppositely detuned laser fields, discussed in Sec. 3.5. Due to the cancellation of the dynamical phase in our scheme, the final state of the atom differs from the initial state of the atom only by the acquired Berry phase. Therefore, the scattering picture is determined only by the Berry phase, which in our case depends not only on the internal, but also on the external degrees of freedom of the atom.

Cancellation of the dynamical phase is one of the novel and important features of the proposed scheme of atomic scattering by two consecutive opposite detuned standing waves. Dynamical phase cancellation allows for more credible and easy measurement of the geometric phase. In our proposal, the Berry phase can be observed by the narrowing of the wave-packet of the atoms prepared initially in the ground state as shown in Sec. 3.6. This novel suggestion of the Berry phase based atomic lens not only beneficially differs from the previous interferometric schemes of the geometric phase observation, but also is applicable to the atomic lithography using processes.

We have considered the atomic scattering by a near-resonant running wave in Ch. 5. Here we take the kinetic energy operator into account and derive formula for the

geometric and dynamical phases. However, as the geometric phase does not depend on the atomic external degrees of freedom, unlike the standing wave case, there exist no base for making an atomic lens. Here we can only use the standard interferometric scheme for observation of the geometric phase. However, the novel scheme of the cancellation of the dynamical phase is proposed also for the running wave.

We emphasize, that the formula obtained for the case of the running wave are reducible to one obtained for the standing wave case, however the dependence on the atomic external degrees of freedom occur only in the case of the standing wave. We provide an extensive comparison of this two cases in Sec. 5.4. The difference between these two proposals occur due to the different time scala used in these cases. The applicability of the Raman-Nath regime is restricted to the small time of interaction τ, that to the fulfillment of the condition $\tau \ll /\sqrt{\omega_{rec}\Omega_0}$. In this case, we are allowed to neglect the kinetic energy operator. The latter, has to be taken into account though, when the inequality $\sqrt{\omega_{rec}\Omega_0} \ll \tau \ll 1/\Gamma$ holds. Here, we are not in the Raman-Nath regime. Hence, the main factor, determining the difference between the considered cases of scattering on the running and standing waves, is the time scale. Taking the kinetic energy operator into account in the case of standing wave is making the system hard to solve analytically. Nevertheless, as we have shown that the formula of the running wave case, where we did take the kinetic energy operator into account, transforms into the formula analogous to those of the standing wave case, we might deduce, that taking the kinetic energy operator into account in the case of the atomic scattering on the standing wave will not change the structure of the expressions for the dynamical and geometric phases significantly from those we obtained in the Raman-Nath regime.

We present the WKB analysis as an independent method to verify the results obtained within the Berry's approach in Sec. 4.1. Here we show that the results within these two approaches coincide. Therefore, we have verified that the Berry's approach is applicable for the scattering of the two-level atom by the electromagnetic wave. We demonstrate the comparison between the dressed state and atomic state approaches in Sec. 4.2 in the weak field limit. Although the results for the ground state probability amplitudes coincide within the two approaches, the excited state probability amplitude can not be determined correctly in the atomic state approach due to the approximations need to be done in the latter case. In Sec. 5.3, we demonstrate that the probability amplitudes obtained within the exact solution of the hypergeometric equation in the case of the inverse cosh envelope coincide with those obtained within the Berry's formalism. This verifies again the applicability of the Berry's geometric phase approach to the atomic scattering. However, we emphasize the power and generality of the Berry's approach as it is valid for any envelope. On a contrary, the exact solution through the hypergeometric functions is available only in the inverse-cosh shape of the envelope.

We demonstrate the applicability of the Berry's approach to the case of the atomic scattering by the electromagnetic field and propose a novel scheme of the dynamical phase cancellation, based on the dynamical phase antisymmetry in the detuning sign and the geometric phase symmetry in it. Moreover, we propose a novel scheme of geometric phase observation in the atomic scattering by the standing wave in the Raman-Nath regime (time of interaction is small). Here, the atomic lens based on the atomic-position dependence of the geometric phase is introduced as a novel approach to the geometric phase measurement. The measurable narrowing of the atomic wave-packet here is determined by the geometric phase due to the dependence of the latter on the atomic external degrees of freedom, such as the position of the atom. When the interaction time is large, we are not in the Raman-Nath regime anymore, and the geometric phase observation is possible only in the standard interferometric experiment, while this geometric phase does not depend on the position of the atom.

Appendix A

Flux through infinitely many windings

In this appendix we evaluate the flux through the area in parameter space defined by the trajectory following from the Eckart envelope of the electromagnetic field, Eq. (3.75). In contrast to the mesa and squared-cos-envelopes, where the paths circumvent the origin of parameter space only once, we now have infinitely many windings. Here the separation of the trajectory from the origin, determined by the strength of the envelope, first increases from zero to a maximum value and then decreases again to zero. As a result, we obtain infinitely many areas each of different size.

In order to perform the integration in the equation Eq. (3.75) we now need to determine the angles ϕ corresponding to the path defining the m-th area. This path originates from the envelope in the time intervals $-t_m \leq t \leq -t_{m-1}$ and $t_{m-1} \leq t \leq t_m$, where $t_m \equiv m\pi/\omega_\alpha$, as shown by Fig. A.1. According to Eq. (3.53) these times define the moments where the trajectory crosses the symmetry axis of the cardioids. Since $\phi = \omega_\alpha t$ these time domains translate into the integration intervals $-\phi_m \leq \phi \leq -\phi_{m-1}$ and $\phi_{m-1} \leq \phi \leq \phi_m$ with $\phi_m \equiv m\pi$.

Hence, the geometrical phase $\gamma^{(m)}$ given by the flux through the m-th area reads

$$\gamma^{(m)} = \frac{1}{2}\left[\int_{-m\pi}^{-(m-1)\pi} \mathrm{d}\phi \left(\frac{\cosh(\phi/(\omega_\alpha\tau))}{\sqrt{\cosh^2(\phi/(\omega_\alpha\tau)) + a^2}} - 1\right) + \int_{(m-1)\pi}^{m\pi} \mathrm{d}\phi \left(\frac{\cosh(\phi/(\omega_\alpha\tau))}{\sqrt{\cosh^2(\phi/(\omega_\alpha\tau)) + a^2}} - 1\right)\right], \tag{A.1}$$

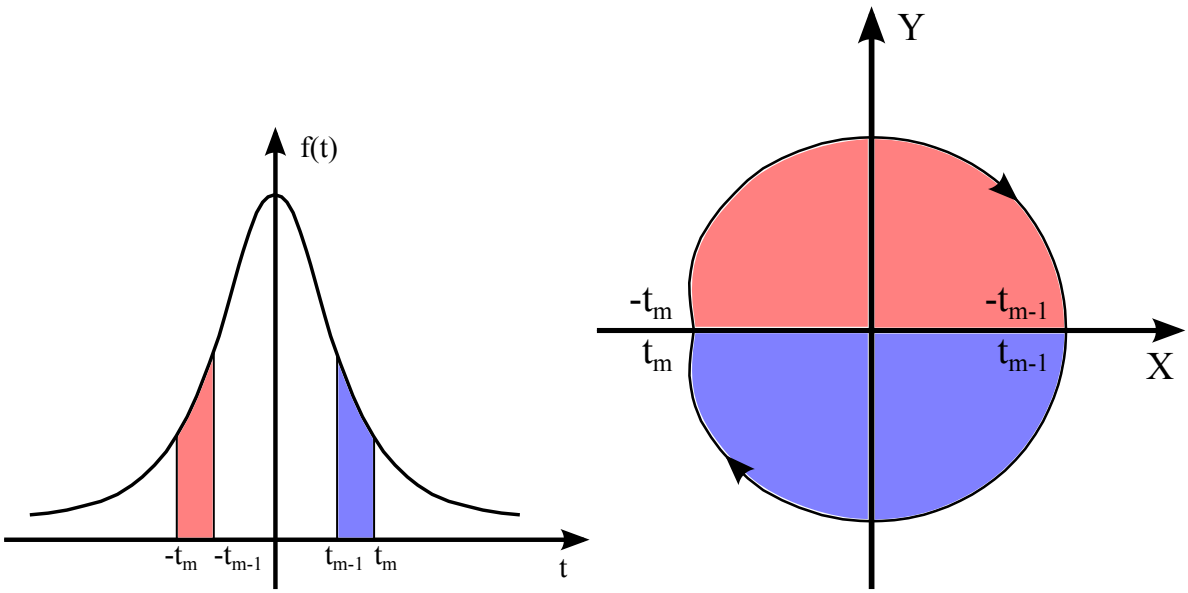


Figure A.1: Translation of field envelope $f = f(t)$ during two symmetrically located time intervals (left) into a closed circuit in parameter space. The m-th cardioid (right) arises from the envelope $f = f(t)$ during the time intervals $-t_m \leq t \leq -t_{m-1}$ and $t_{m-1} \leq t \leq t_m$.

which due to the symmetry of the integrand simplifies to

$$\gamma^{(m)} = \omega_\alpha \tau \int_{\theta_{m-1}}^{\theta_m} \mathrm{d}\theta \left[\frac{\cosh\theta}{\sqrt{\cosh^2\theta + a^2}} - 1 \right], \tag{A.2}$$

where we have introduced the integration variable $\theta \equiv \phi/(\omega_\alpha\tau)$ and $\theta_m \equiv m\pi/(\omega_\alpha\tau)$.

With the help of the integral relation, Eq. (3.78), we find the expression

$$\gamma^{(m)} = \omega_\alpha \tau \left[\ln \frac{F_m}{F_{m-1}} - \frac{\pi}{\omega_\alpha \tau} \right], \tag{A.3}$$

where we have introduced the abbreviation

$$F_m \equiv \sinh\theta_m + \sqrt{\cosh^2\theta_m + a^2}. \tag{A.4}$$

Thus, the total geometric phase is the sum of the fluxes through all areas

$$\gamma_E = \sum_{m=1}^{\infty} \gamma^{(m)} = \omega_\alpha \tau \lim_{N\to\infty} \sum_{m=1}^{N} \left[\ln \frac{F_m}{F_{m-1}} - \frac{\pi}{\omega_\alpha \tau} \right]. \tag{A.5}$$

With the help of the functional relation

$$\ln \frac{F_m}{F_{m-1}} = \ln F_m - \ln F_{m-1} \tag{A.6}$$

of the logarithm the expression for the Berry phase Eq. (A.5) takes the form

$$\begin{aligned}\gamma_E &= \omega_\alpha \tau \lim_{N\to\infty} \left\{ \ln \left[\prod_{m=1}^{N} \frac{F_m}{F_{m-1}} \right] - N \frac{\pi}{\omega_\alpha \tau} \right\} \\ &= \omega_\alpha \tau \lim_{N\to\infty} \left[\ln \frac{F_N}{F_0} - N \frac{\pi}{\omega_\alpha \tau} \right]. \end{aligned} \tag{A.7}$$

Recalling the asymptotic behavior

$$\sinh\theta \cong \cosh\theta \cong \frac{1}{2} \mathrm{e}^{\theta} \tag{A.8}$$

in the limit of $\theta \to \infty$ we find

$$F_N \cong \exp\left(N \frac{\pi}{\omega_\alpha \tau} \right) \tag{A.9}$$

which together with

$$F_0 = \sqrt{1+a^2} \tag{A.10}$$

yields

$$\gamma_E = \omega_\alpha \tau \ln \sqrt{1+a^2}. \tag{A.11}$$

We conclude by noting that we also arrive at Eq. (A.11) by substituting the expression Eq. (A.2) for $\gamma^{(m)}$ into the sum Eq.(A.5). Indeed, in this case we find

$$\gamma_E = \omega_\alpha \tau \sum_{m=1}^{\infty} \int_{\theta_{m-1}}^{\theta_m} \mathrm{d}\theta \left[\frac{\cosh\theta}{\sqrt{\cosh^2\theta + a^2}} - 1 \right], \tag{A.12}$$

which with the help of the identity

$$\sum_{m=1}^{\infty} \int_{\theta_{m-1}}^{\theta_m} \mathrm{d}\theta g(\theta) = \int_{\theta_0}^{\theta_\infty} \mathrm{d}\theta g(\theta) \tag{A.13}$$

together with $\theta_0 = 0$ and $\theta_\infty = \infty$ leads us to Eq. (3.76)

Bibliography

[1] M. V. Berry, *Quantal phase factors accompanying adiabatic changes*, Proc. R. Soc. London A **392**, 45–57 (1984).

[2] M. Berry, *The geometric phase*, Scientific American **259**, 46–52 (1988).

[3] A. Shapere and F. Wilczek, "Geometric Phases in Physics", World Scientific, Singapore (1989).

[4] M. Berry, *Geometric phase memories*, Nature Physics **6**, 148–150 (2010).

[5] A. Bohm, "Quantum mechanics: Foundations and Applications", Springer, New York (1993).

[6] J. W. Zwanziger, M. Koenig and A. Pines, *Berry's Phase*, Annual Review of Physical Chemistry **41**, 601–646 (1990).

[7] J. Anandan, *The geometric phase*, Nature **360**, 307–313 (1992).

[8] A. Bohm, A. Mostafazadeh, H. Koizumi, Q. Niu and J. Zwanziger, "The geometric phase in quantum systems. Foundations, mathematical concepts, and applications in molecular and condenced matter physics.", Springer, Berlin Heidelberg (2003).

[9] J. Anandan, J. Christian and K. Wanelik, *Resource Letter GPP-1: Geometric Phases in Physics*, Am. J. Phys. **65**, 180–185 (1997).

[10] M. V. Berry, *Quantum phase corrections from adiabatic iteration*, Proc. R. Soc. London A **414**, 31–46 (1987).

[11] G. Giavarini, E. Gozzi, D. Rohrlich and W. D. Thacker, *On the removability of Berry's phase*, Journal of Physics A: Mathematical and General **22**, 3513–3529 (1989).

[12] H. Kuratsuji, *Geometric Canonical Phase Factors and Path Integrals*, Phys. Rev. Lett. **61**, 1687–1690 (1988).

[13] I. Bialynicki-Birula and Z. Bialynicka-Birula, *Berry's phase in the relativistic theory of spinning particles*, Phys. Rev. D **35**, 2383–2387 (1987).

[14] A. Tomita and R. Y. Chiao, *Observation of Berry's Topological Phase by Use of an Optical Fiber*, Phys. Rev. Lett. **57**, 937–940 (1986).

[15] R. Y. Chiao and Y. S. Wu, *Manifestations of Berry's Topological Phase for the Photon*, Phys. Rev. Lett. **57**, 933–936 (1986).

[16] T. Bitter and D. Dubbers, *Manifestation of Berry's topological phase in neutron spin rotation*, Phys. Rev. Lett. **59**, 251–254 (1987).

[17] Y. Hasegawa, R. Loidl, M. Baron, G. Badurek and H. Rauch, *Off-Diagonal Geometric Phase in a Neutron Interferometer Experiment*, Phys. Rev. Lett. **87**, 070401 (2001).

[18] S. Filipp, Y. Hasegawa, R. Loidl and H. Rauch, *Noncyclic geometric phase due to spatial evolution in a neutron interferometer*, Phys. Rev. A **72**, 021602 (2005).

[19] S. Filipp, J. Klepp et al., *Experimental Demonstration of the Stability of Berry's Phase for a Spin-1/2 Particle*, Phys. Rev. Lett. **102**, 030404 (2009).

[20] S. Sponar, J. Klepp et al., *New aspects of geometric phases in experiments with polarized neutrons*, Journal of Physics A: Mathematical and Theoretical **43**, 354015 (2010).

[21] D. Suter, G. C. Chingas, R. Harris and A. Pines, *Berry's phase in magnetic resonance*, Mol. Phys. **61**, 1327–1340 (1987).

[22] D. J. Richardson, A. I. Kilvington, K. Green and S. K. Lamoreaux, *Demonstration of Berry's Phase Using Stored Ultracold Neutrons*, Phys. Rev. Lett. **61**, 2030–2033 (1988).

[23] D. H. Kobe, V. C. Aguilera-Navarro, S. M. Kurcbart and A. H. Zimerman, *Exact phases and probabilities for a spin-1/2 particle in a precessing magnetic field*, Phys. Rev. A **42**, 3744–3750 (1990).

[24] Y. Hasegawa, M. Zawisky, H. Rauch and A. I. Ioffe, *Geometric phase in coupled neutron interference loops*, Phys. Rev. A **53**, 2486–2492 (1996).

[25] C. L. Webb, R. M. Godun et al., *Measurement of Berry's phase using an atom interferometer*, Phys. Rev. A **60**, R1783–R1786 (1999).

[26] J. A. Jones, V. Vedral, A. Ekert and G. Castagnoli, *Geometric quantum computation using nuclear magnetic resonance*, Nature **403**, 869–871 (2000).

[27] D. Leibfried, B. DeMarco et al., *Experimental demonstration of a robust, high-fidelity geometric two ion-qubit phase gate*, Nature **422**, 412–415 (2003).

[28] Y. Aharonov and D. Bohm, *Significance of Electromagnetic Potentials in the Quantum Theory*, Phys. Rev. **115**, 485–491 (1959).

[29] M. Berry, *Anticipations of the geometric phase*, Physics Today **43**, 34–40 (1990).

[30] B. Markovski and S. I. Vinitsky, "Topological phases in quantum theory", World Scientific, Singapore (1989).

[31] M. Berry, *Pancharatnam, virtuoso of the Poincaré sphere: an appreciation*, Current Science **67**, 220–223 (1994).

[32] S. Pancharatnam, *Geometric theory of interference and its applications*, Proc. Ind. Acad. Sci A **44**, 247–262 (1956).

[33] D. Chruściński and A. Jamiołkowski, "Geometric phases in classical and quantum mechanics", Birkhäuser, Boston (2004).

[34] B. Simon, *Holonomy, the Quantum Adiabatic Theorem, and Berry's Phase*, Phys. Rev. Lett. **51**, 2167–2170 (1983).

[35] J. Samuel and R. Bhandari, *General Setting for Berry's Phase*, Phys. Rev. Lett. **60**, 2339–2342 (1988).

[36] A. O. Barut, M. Božić, S. Klarsfeld and Z. Marić, *Measurement of time-dependent quantum phases*, Phys. Rev. A **47**, 2581–2591 (1993).

[37] J. H. Hannay, *The Berry phase for spin in the Majorana representation*, Journal of Physics A: Mathematical and General **31**, L53–L59 (1998).

[38] F. Keck, H. J. Korsch and S. Mossmann, *Unfolding a diabolic point: a generalized crossing scenario*, Journal of Physics A: Mathematical and General **36**, 2125–2137 (2003).

[39] J. W. Zwanziger, S. P. Rucker and G. C. Chingas, *Measuring the geometric component of the transition probability in a two-level system*, Phys. Rev. A **43**, 3232–3240 (1991).

[40] D. J. Moore and G. E. Stedman, *Adiabatic and nonadiabatic Berry phases for two-level atoms*, Phys. Rev. A **45**, 513–519 (1992).

[41] S. J. Wang, *Nonadiabatic Berry's phase for a spin particle in a rotating magnetic field*, Phys. Rev. A **42**, 5107–5110 (1990).

[42] Y. Aharonov and J. Anandan, *Phase change during a cyclic quantum evolution*, Phys. Rev. Lett. **58**, 1593–1596 (1987).

[43] A. G. Wagh, V. C. Rakhecha, P. Fischer and A. Ioffe, *Neutron Interferometric Observation of Noncyclic Phase*, Phys. Rev. Lett. **81**, 1992–1995 (1998).

[44] B. C. Sanders, H. Guise, S. D. Bartlett and W. Zhang, *Geometric Phase of Three-Level Systems in Interferometry*, Phys. Rev. Lett. **86**, 369–372 (2001).

[45] M. S. Sarandy and D. A. Lidar, *Abelian and non-Abelian geometric phases in adiabatic open quantum systems*, Phys. Rev. A **73**, 062101 (2006).

[46] A. Zee, *Non-Abelian gauge structure in nuclear quadrupole resonance*, Phys. Rev. A **38**, 1–6 (1988).

[47] N. Manini and F. Pistolesi, *Off-Diagonal Geometric Phases*, Phys. Rev. Lett. **85**, 3067–3071 (2000).

[48] S. M. Barnett, D. Ellinas and M. A. Dupertuis, *Berry's phase in the coherent excitation of atoms*, J. Mod. Opt. **35**, 565 (1988).

[49] S. P. Tewari, *Berry's phase in a two-level atom*, Phys. Rev. A **39**, 6082–6085 (1989).

[50] A. Aguiar Pinto, M. Moutinho and M. Thomaz, *Berry's phase in the two-level model*, Braz. J. Phys. **39**, 326-330 (2009).

[51] D. Ellinas, S. M. Barnett and M. A. Dupertuis, *Berry's phase in optical resonance*, Phys. Rev. A **39**, 3228–3237 (1989).

[52] T. Sen and J. L. Milovich, *Geometric phases in two-level atoms excited by pulses propagating without loss*, Phys. Rev. A **45**, 1371–1388 (1992).

[53] G. De Chiara and G. M. Palma, *Berry Phase for a Spin* 1/2 *Particle in a Classical Fluctuating Field*, Phys. Rev. Lett. **91**, 090404 (2003).

[54] X. Wang and K. Matsumoto, *NMR C-NOT gate through the Aharanov-Anandan phase shift*, Journal of Physics A: Mathematical and General **34**, L631 (2001).

[55] G. Florio, P. Facchi, R. Fazio, V. Giovannetti and S. Pascazio, *Robust gates for holonomic quantum computation*, Phys. Rev. A **73**, 022327 (2006).

[56] D. Møller, L. B. Madsen and K. Mølmer, *Geometric phase gates based on stimulated Raman adiabatic passage in tripod systems*, Phys. Rev. A **75**, 062302 (2007).

[57] M. Reich, U. Sterr and W. Ertmer, *Scheme for measuring a Berry phase in an atom interferometer*, Phys. Rev. A **47**, 2518–2522 (1993).

[58] M. A. Ol'shaniî, *Berry-phase-induced achromatic plate for atomic interferometry*, *Phys. Lett.* A **186**, 369-374 (1994).

[59] W. Schleich, "Quantum Optics in Phase Space", WILEY-VCH Verlag, Berlin (2002).

[60] P. Ehrenfest, *Bemerkung betreffs der spezifischen Wärme zweiatomiger Gase*, Verh. D. physik. Ges. **15**, 451 (1913).

[61] M. Born and V. Fock, *Beweis des Adiabatensatzes*, Zeitschrift für Physik **51**, 165–180 (1928).

[62] B. Van Der Waerden, "Sources of quantum mechanics", Dover Publications, New York (1968).

[63] P. Ehrenfest, *A theorem of Boltzmann and its connection with the theory of quanta*, Proc. Kon. Akad. Amsterdam **16**, 591 (1913).

[64] P. Ehrenfest, *Adiabatic invariants and the theory of quanta*, Philosophical Magazine Series 6 **33**, 500 (1917).

[65] M. Born, *Das Adiabatenprinzip in der Quantenmechanik*, Zeitschrift für Physik **40**, 167–192 (1926).

[66] A. Messiah, "Quantum mechanics", Dover Publications, New York (1999).

[67] L. Schiff, "Quantum mechanics", McGraw-Hill Book Company, Inc., New York (1968).

[68] P. Morse and H. Feshbach, "Methods of Theoretical Physics, Part I and Part II", McGraw-Hill Book Company, Inc., New York (1953).

[69] A. P. Kazantsev, G. Surdutovich and V. Yakovlev, "Mechanical Action of Light on Atoms", World Scientific, Singapore (1990).

[70] M. Sargent III and P. Meystre, "Elements of Quantum Optics", Springer, Berlin Heidelberg (1990).

[71] L. Mandel and E. Wolf, "Optical coherence and quantum optics", Cambridge University Press, Cambridge (1995).

[72] P. Lambropoulos and D. Petrosyan, "Fundamentals of Quantum Optics and Quantum Information", Springer, Berlin Heidelberg (2007).

[73] C. Cohen-Tannouji, J. Dupont-Roc and G. Grynberg, "Photons and Atoms. Introduction to Quantum Electrodynamics", John Wiley & Sons, Inc., New York (1989).

[74] C. Cohen-Tannouji, J. Dupont-Roc and G. Grynberg, "Atom–Photon interactions. Basic processes and applications", John Wiley & Sons, Inc., New York (1992).

[75] P. Meystre, "Atom Optics", Springer, New York (2001).

[76] L. Allen and J. Eberly, "Optical resonance and two-level atoms", John Wiley & Sons, Inc., New York (1975).

[77] A. Erdélyi, "Higher Transcendental Functions", McGraw-Hill Book Company, Inc., New York (1953).

[78] M. Abramowitz and I. A. Stegun, "Handbook of mathematical functions", Dover Publications, Inc., New York (1972).

[79] A. Prudnikov, Y. A. Brychkov and O. I. Marichev, "Integrals and Series", Gordon and Breach Science Publishers, New York (1992).

[80] I. S. Gradshteyn and I. M. Ryzhik, "Table of Integrals, Series, and Products", Academic Press, New York (1965).

[81] M. Fedorov, "Atomic and free electrons in a strong light field", World Scientific, Singapore (1997).

Zusammenfassung

Das Konzept der geometrische Phase beruht auf einem zeitabhängigen Hamiltonian, dessen Parameter sich langsam mit der Zeit ändern. Bei zyklischer Änderung der Parameter, d.h. wenn der Hamiltonian zu seiner Anfangsform zurückgekehrt ist, kehren die Eigenzustände nicht unbedingt zum Anfangswert zurück, sondern können eine Phase aufnehmen. Dieses Phänomen wurde in Experimenten mit polarisiertem Licht, Radiowellen, Molekülen, u.s.w. beobachtet. Der Aharonov-Bohm Effekt ist das hervorstechendste Beispiel. Außerdem können viele bekannte Phänomene, wie das Foucault'sche Pendel oder die Präzession des Neutrons im magnetische Feld, mittels der geometrischen Phase beschrieben werden.

Umfangreiche theoretische und experimentelle Forschung fand in den Bereichen der Quantenholonomie, adiabatischen und nicht-adiabatischen, zyklischen und nicht-zyklischen, Abel'schen und nicht-Abel'schen, sowie der nicht-diagonalen geometrischen Phase statt. Außerdem treten die Effekte der geometrischen Phasen in der kohärenten Anregung der Atomen auf. Darüber hinaus sind geometrische Phasen relativ unempfindlich gegen spezifische Arten des Rauschens und demzufolge hilfreich bei der Verwirklichung robuster Quantengatter. Es gibt verschiedene Vorschläge für die Messung der geometrischen Phasen in der Atominterferometrie. Dennoch wurde bisher nur die Abhängigkeit von den atomaren internen Freiheitsgraden untersucht. In dieser Arbeit wurde dieser Zugang um die Verwendung externer Freiheitsgraden des Atoms erweitert.

Wir schlagen ein Beobachtungsschema für die geometrische Phase, die während der Wechselwirkung mit den Streufeld erworben wird, vor. Innerhalb der Raman-Nath Näherung der Bewegung des atomaren Massenmittelpunkts, sowie adiabatischem Ein– und Ausschalten der Wechselwirkung und der Dreh-Wellen-Näherung erhalten wir eine Bedingung für die Auflösung der dynamischen Phase und zeigen, dass das Streuungs-Bild von der von externen Parametern abhängigen geometrischen Phase bestimmt ist. Außerdem schlagen wir ein neuartiges Schema der Beobachtung der geometrischen Phase durch die Errichtung der atomischen Linse vor.

Dafür betrachten wir die Streuung eines zwei-Niveau Atoms an einer stehenden Welle, die aus zwei gegenläufigen Wellen mit gleicher Amplitude und Frequenz gebildet

wird. Dabei sind die Ausbreitungsrichtungen leicht gegeneinander verschoben und die Frequenz des elektromagnetisches Feldes ist gegenüber der Resonanzfrequenz des Atoms verstimmt. Die vom Atom bei der Streuung aufgesammelten Phasen lassen sich in die dynamische und die geometrische Phase unterteilen. Die dynamische Phase ist antisymmetrisch bezüglich der Verstimmung, die geometrische hingegen symmetrisch. Dementsprechend kann durch zwei aufeinanderfolgende Streusysteme, die sich nur im Vorzeichen der Verstimmung unterscheiden, die dynamische Phase eliminiert und die geometrische verdoppelt werden. Das hat den Vorteil, dass die wesentlich kleinere geometrische Phase leichter zu beobachten ist. Unser Streuschema wirkt auf ein aus in Grundzustand präparierten Atomen wie eine atomare Linse, d.h. die Berry Phase läßt sich mittels der Fokusierung des Wellenpakets bestimmen. Dementsprechend ist die geometrische Phase in dem Gebiet der Lithografie mit kalten Atomen nutzbar.

Publications

1. P.V. Mironova, M.A. Efremov, W.P. Schleich, "Berry phase in atom optics", 2010 (in preparation for *Phys. Rev. A*)

2. V.V. Chernushkin, P.V. Mironova and V.D. Ovsiannikov, "Magnetoelectric Jones spectroscopy of alkali atoms", *J. Phys. B: At. Mol. Opt. Phys.* 2008 **41** (11) 115401

3. P.V. Mironova, V.D. Ovsiannikov, V.V. Chernushkin, "Magnetoelectric Jones birefringence and dichroism in a medium of free atoms", *J. Phys. B: At. Mol. Opt. Phys.*, 2006, **39** (23), 4999

4. P.V. Mironova, V.D. Ovsiannikov, V.V. Tchernoushkine, "Interference of $E2$ and $M1$ $n_1^2P - n_2^2P$ transition amplitudes in steady-field-induced coherent mixing of two resonant waves on atoms", *J. Phys. B: At. Mol. Opt. Phys.*, 2005, **38** (15), 2467

5. P.V. Mironova, V.D. Ovsiannikov, V.V. Tchernoushkine, "$E2/M1$ Amplitude Ratio in Dipole-Forbidden Transitions of Alkali Atoms from Two-Wave Mixing", *Laser Phys.*, 2005, **15** (4), 492

6. P.V. Mironova, V.D. Ovsiannikov, N.V. Pershin, E.V. Chaplygin, "The $E2/M1$ amplitude ratio in a dc-field-induced two-laser-wave mixing in atoms", *Quantum Electron.*, 2004, **34** (5), 422

Posters and Talks

1. SFB/TRR 21 International Conference, Workshop 2010, 28 November – 2 December 2010, Schloss Reisensburg, Günzburg, Germany (Poster)

2. DPG Frühjahrstagung des Arbeitskreises Atome, Moleküle, Quantenoptik und Plasmen (AMOP), 8.–12. März 2010, Hannover, Germany (Talk)

3. SFB/TRR 21 International Conference, Workshop 2009, 15–19 November 2009, Schloss Reisensburg, Günzburg, Germany (Poster)

4. 443. WE-Heraeus workshop "Quantum Simulators", 12–15 Oktober 2009, Bad Honnef, Germany (Poster)

5. 16th Central European Workshop on Quantum Optics, 23–27 May 2009, Turku, Finland (Poster)

6. DPG Frühjahrstagung des Arbeitskreises Atome, Moleküle, Quantenoptik und Plasmen (AMOP), 2.–6. März 2009, Hamburg, Germany (Talk)

7. SFB/TRR 21 International Conference, Workshop 2008, 2–6 December 2008, Schloss Reisensburg, Günzburg, Germany (Poster)

8. 5th Central European Quantum Information Processing Workshop 5–8 June 2008, Telc, Czech Republic (Poster)

9. International Workshop on modern trends in quantum optics and quantum information, Prague, Czech Republic, May 1–4, 2008 (Poster)

10. DPG Frühjahrstagung des Arbeitskreises Atome, Moleküle, Quantenoptik und Plasmen (AMOP), 10.–14. März 2008, Darmstadt, Germany (Poster)

11. Young European Physicists meeting 2007, 17–21 September 2007, Frauenchiemsee, Germany (Talk)

12. 4th Central European Quantum Information Processing Workshop, 24–27 June 2007, Valtice, Czech Republic (Talk)

13. DPG Frühjahrstagung des Arbeitskreises Atome, Moleküle, Quantenoptik und Plasmen (AMOP), 19.–23. März 2007, Düsseldorf, Germany (Poster)

14. Young European Physicists meeting 2006, 11-15 December 2006, Budmerice, Slovakia (Talk)

Danksagung

An dieser Stelle möchte ich mich recht herzlich bedanken bei allen, die das Erscheinen dieser Arbeit ermöglicht haben.

Als erstes gebührt Herrn Prof. Dr. W.P. Schleich Dank, der mich als Doktorandin an sein Institut genommen hat und dessen physikalische Intuition, tiefe Kenntnise und klare Visionen von Zusammenhängen zwischen allen möglichen physikalischen Problemen, sein Weitblick und seine Liebe zum Detail, sein unglaubliches wissenschaftliches Charisma und sein Talent zur einfachen Darstellung komplizierter physikalischen Fragen mich immer fasziniert und inspiriert haben. Er und seine wunderbare Frau Kathy Dodson-Schleich, deren Warmherzigkeit und Güte ich nie vergessen werde, haben eine unglaublich freundliche Atmosphäre am Institut geschaffen, in dem man sich sofort zu Hause fühlt. Danke sehr Euch beiden für alles, was dieses "Quantenfamilie"-Gefühl uns Mitarbeitern des Institutes gibt!

Als nächstes möchte ich Herrn Dr. Maxim Efremov danken für die Öffenheit zum Diskutieren, für die Betreuung, Hilfe mit Rat und Tat während meiner Forschungsarbeit. Seine erstaunlichen physikalischen Kenntnise und sein kritischer Blick an all die Probleme haben sehr zu den Ergebnissen dieser Arbet beigetragen.

Ich bedanke mich herzlichst bei Herrn Prof. V.P. Yakovlev und Herrn Prof. M.V. Fedorov für zahlreiche Diskussionen und Ratschläge.

Ich möchte mich sehr gerne für die Freundlichkeit und Zuverlässigkeit bei all meinen lieben Kollegen bedanken. Viele von ihnen sind echte Freunde geworden. Danke sehr, Conny, Steffi, Piroska, Parimah, Christof, Sabine, Michael Bußhardt, Michael Grupp, Daniela, Carsten, Bettina, Rüdiger, Sarah und Endre, Dennis, Paul und alle anderen! Ich möchte mich besonders bedanken bei all den Leuten, die sich beim Korrekturlesen dieser Arbeit beteiligt haben. Conny, Christof, Rüdiger, Sabine, Kedar, Michael Buser, Michael Grupp, Rainer, Danke sehr für eure Mühe, unzählige hilfreiche Kommentare und Hinweise! Ich bedanke mich bei Herrn Dr. Roman Nolte fürs Korrekturlesen der deutschen Zusammenfassung recht herzlich!

Ihr alle wart eine liebe "Quantenfamilie" in all den vier Jahren!

Danke liebe "russische" Kollegen: Andrei, Lev, Maxim! Ich konnte jeden Tag mal wieder meine Muttersprache hören und sprechen. Es war sehr nett!

Ich danke meiner lieben Freundin Alexandra Magdalene Liguori vielmals. Liebe ALEx, die Unterstützung deiner Freundschaft ist unschätzbar für mich!

Ich bedanke mich auch recht herzlich bei allen meinen Freunden, die mich im Gedächtnis behalten und immer wieder in meiner Heimatstadt herzlich begrüßen. Julia, Elena, Masha und Denis, Tanya, Anton, Danke Euch!

Meine liebe Eltern, meine liebe Familie, ohne Euch wäre ich nie so weit gekommen. Gleich was ich jetzt und wie ich es sage, es wird nie genug sein, um Euch ausreichend danken zu können! Ihr wart immer da, wenn ich Euch brauchte, das heißt jeden Tag meines Lebens. Ihr wart und seid meine Zuhause. Egal, wo ich bin und was ich tue, ich weiß, Ihr werdet mich immer lieb haben, so wie ich Euch. Vielen lieben herzlichen Dank, meine Lieben!